Supernova Overview

2019.3.9 @ Tohoku Univ.
Hideyuki Suzuki, Tokyo Univ. of Science

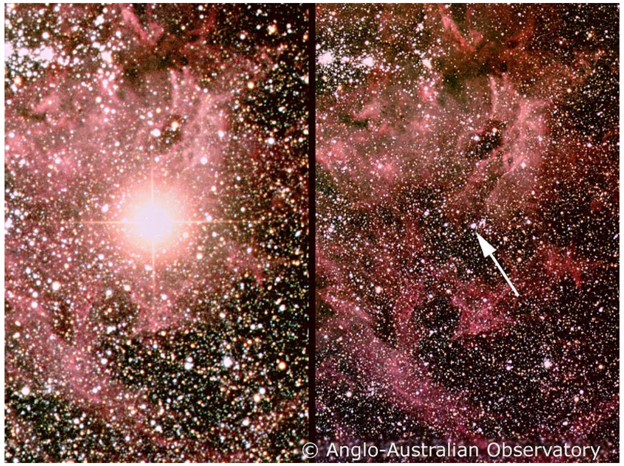

SN1987A

- Overview
- Our research
  main collaborator: K. Nakazato
  - Supernova Neutrino Database
  - Supernova Relic Neutrino Database
  - Togashi EOS
  - Proto Neutron-Star Cooling

Stellar Evolution and Supernovae

mass loss, metallicity, rotation, binary

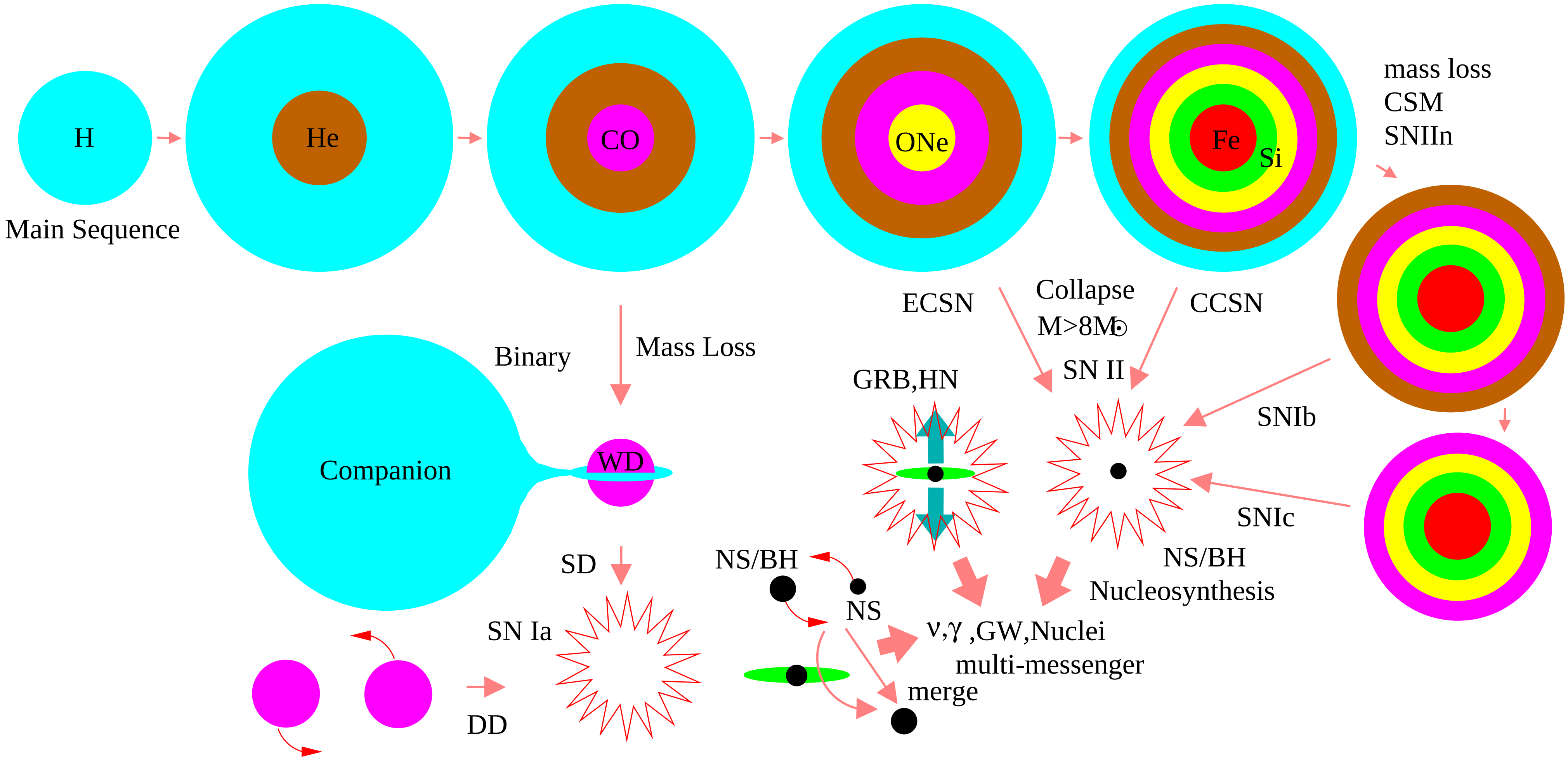

Massive Star ($M > 8M_\odot$)

Main Sequence (H burning) $\Rightarrow$ Onion Skin Structure

$\Rightarrow$ ONe core/"Fe" core + envelope (mass loss might occur)

$\Rightarrow$ Core Collapse $\Rightarrow$ Neutron Star(or Black Hole) + Supernova Explosion

with H envelope (Type II SN), w/o H env.(Type Ib), w/o H/He env.(Type Ic)

Supernova neutrinos can be roughly divided into 3 phases (while they are continuous).

1. collapse and bounce phase: ($O(10)$msec), $O(10^{51})$erg
   core collapse, inner core bounce, shock launch, neutronization burst of $\nu_{\rm e}$
2. accretion phase: ($O(1)$sec), $O(10^{53})$erg
   shock wave propagation, stall, revival (leading to explosion) or BH formation
3. cooling phase: ($O(10) - O(100)$sec), $O(10^{53})$erg
   Proto Neutron Star (PNS) cooling

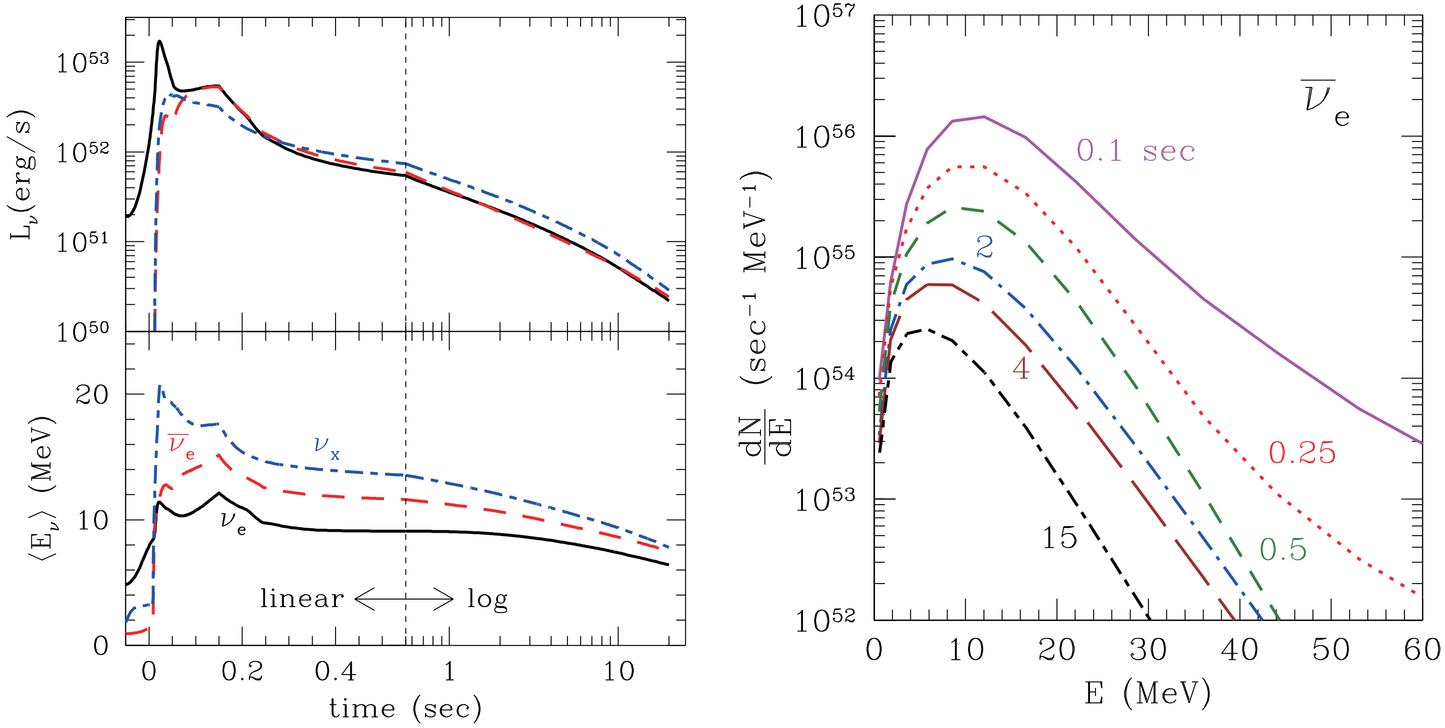

Figure 14. Time evolution of neutrino luminosity and average energy (left) and number spectrum of $\bar{\nu}_e$ (right) from νRHD and PNSC simulations with the interpolation (13) for the model with $(M_{\rm init}, Z, t_{\rm revive}) = (13\,M_\odot, 0.02, 100\ {\rm ms})$. In the left panel, solid, dashed, and dot-dashed lines represent ν_e, $\bar{\nu}_e$, and ν_x (dot-dashed lines), respectively. In the right panel, the lines correspond, from top to bottom, to 0.1, 0.25, 0.5, 2, 4, and 15 s after the bounce.

Nakazato *et al.*, 2013

1. collapse and bounce phase: ($O(10)$msec)
core collapse, inner core bounce, shock launch

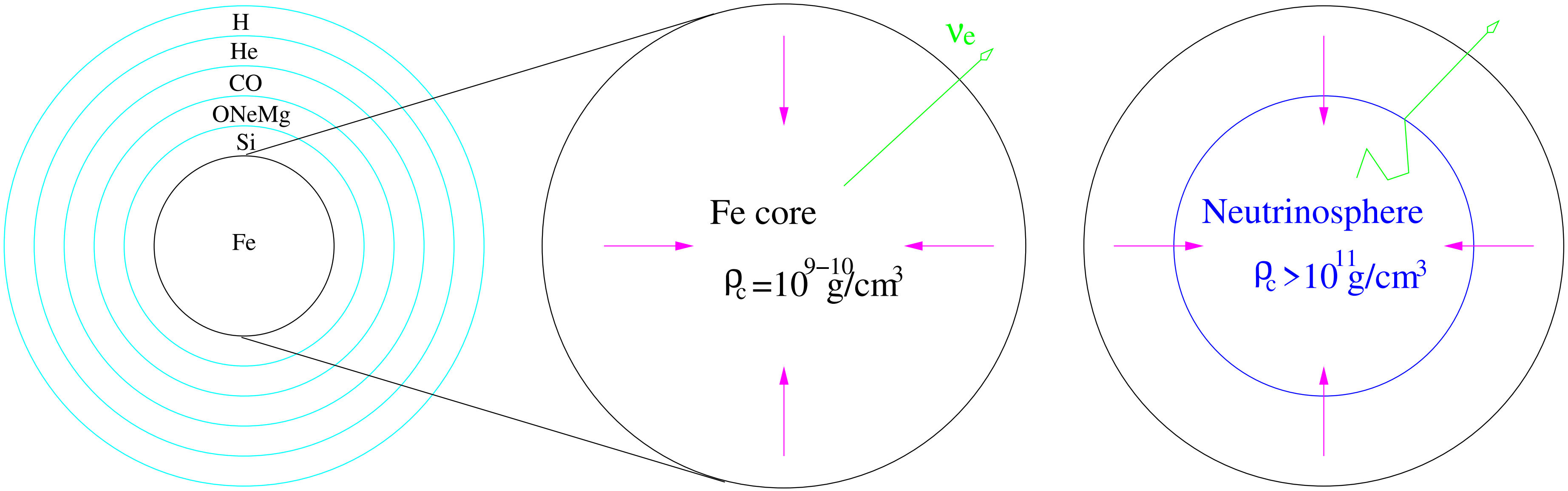

- onset of core collapse: core ($M \sim 1.5 M_\odot$) transparent for neutrinos.
  Neutrino source: electron capture $\mathrm{e}^-\ \mathrm{A}(N,Z) \longrightarrow \nu_\mathrm{e}\ \mathrm{A}'(N+1, Z-1)$ when $\mu_\mathrm{e} + m_A c^2 > m_{A'} c^2$
  Neutrinos: not in thermal/chemical equilibrium with matters.
- neutrino trapping: $\rho_c \gtrsim\ O(10^{11})\mathrm{g/cm}^3$, the core becomes opaque for neutrinos ($\nu_\mathrm{e}\ \mathrm{A} \to \nu_\mathrm{e}\ \mathrm{A}$).
  Inside the neutrinosphere, neutrinos are trapped and diffuse out in time scale of $O(0.1)$-$O(10)$sec.

In this stage, ν_e's due to electron capture dominate.

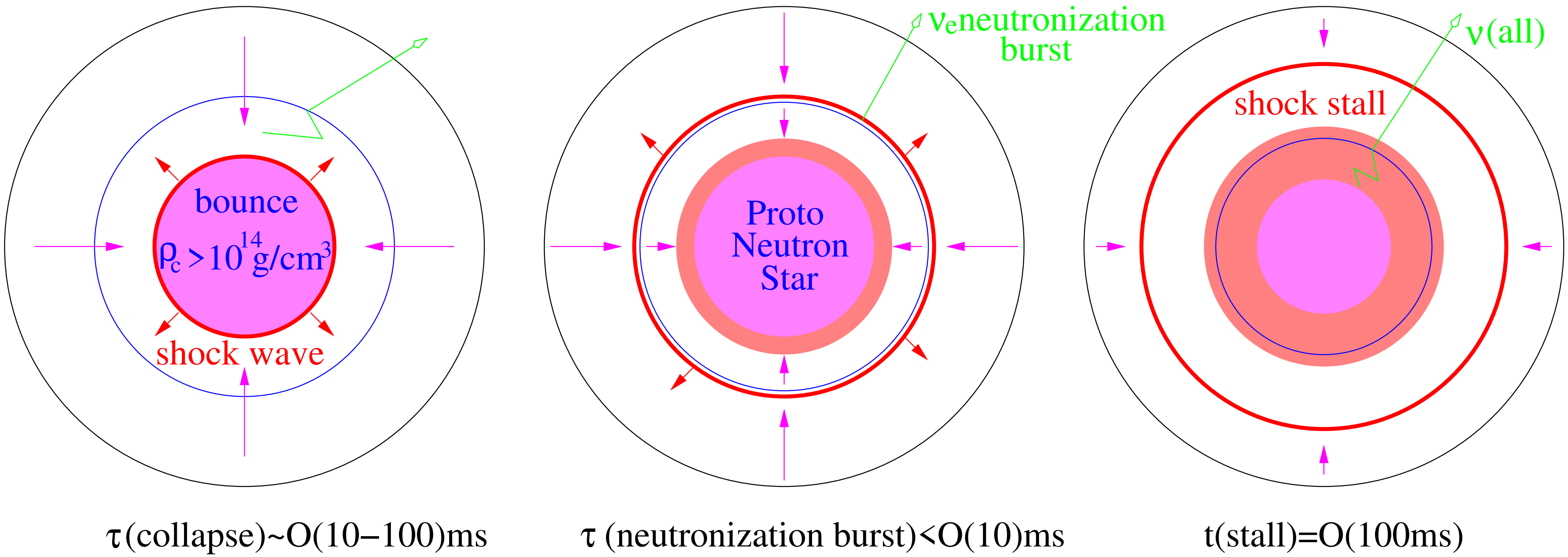

- core bounce: $\rho_c \gtrsim O(10^{14})\mathrm{g/cm}^3$, the inner core bounces, launches a shock wave at the boundary between bounced inner core ($M_{\text{inner core}} \sim 0.5$-$0.8 M_\odot$) and still free-falling outer core.

  $E_{\text{shock}} \sim \frac{G M^2_{\text{inner core}}}{R_{\text{inner core}}} \sim \text{several} \times 10^{51}\text{erg} > E_{\text{explosion}}.$

- neutronization burst of ν_{e}

  shocked region: $\mathrm{A} \to \mathrm{p}, \mathrm{n}$, $\sigma_{\mathrm{e-cap}}(\mathrm{p}) > \sigma_{\mathrm{e-cap}}(\mathrm{A}) \Rightarrow \mathrm{e}^-\mathrm{p} \to \nu_{\mathrm{e}}\mathrm{n}$

  When the shock wave passes the neutrinosphere, the emitted ν_{e}'s behind the shock front can escape from the core immediately

  $\Rightarrow$ **neutronization burst** of ν_{e}.

  $L_{\nu_{\mathrm{e}}} > 10^{53}\text{erg/sec}$, the time scale of the shock propagation through the neutrinosphere $\Delta t \lesssim O(10)\text{msec} \to E_{\nu_{\mathrm{e}}} \sim L_{\nu_{\mathrm{e}}} \Delta t \sim O(10^{51})\text{erg}$

Comparison of different numerical codes (1D Boltzmann solvers)

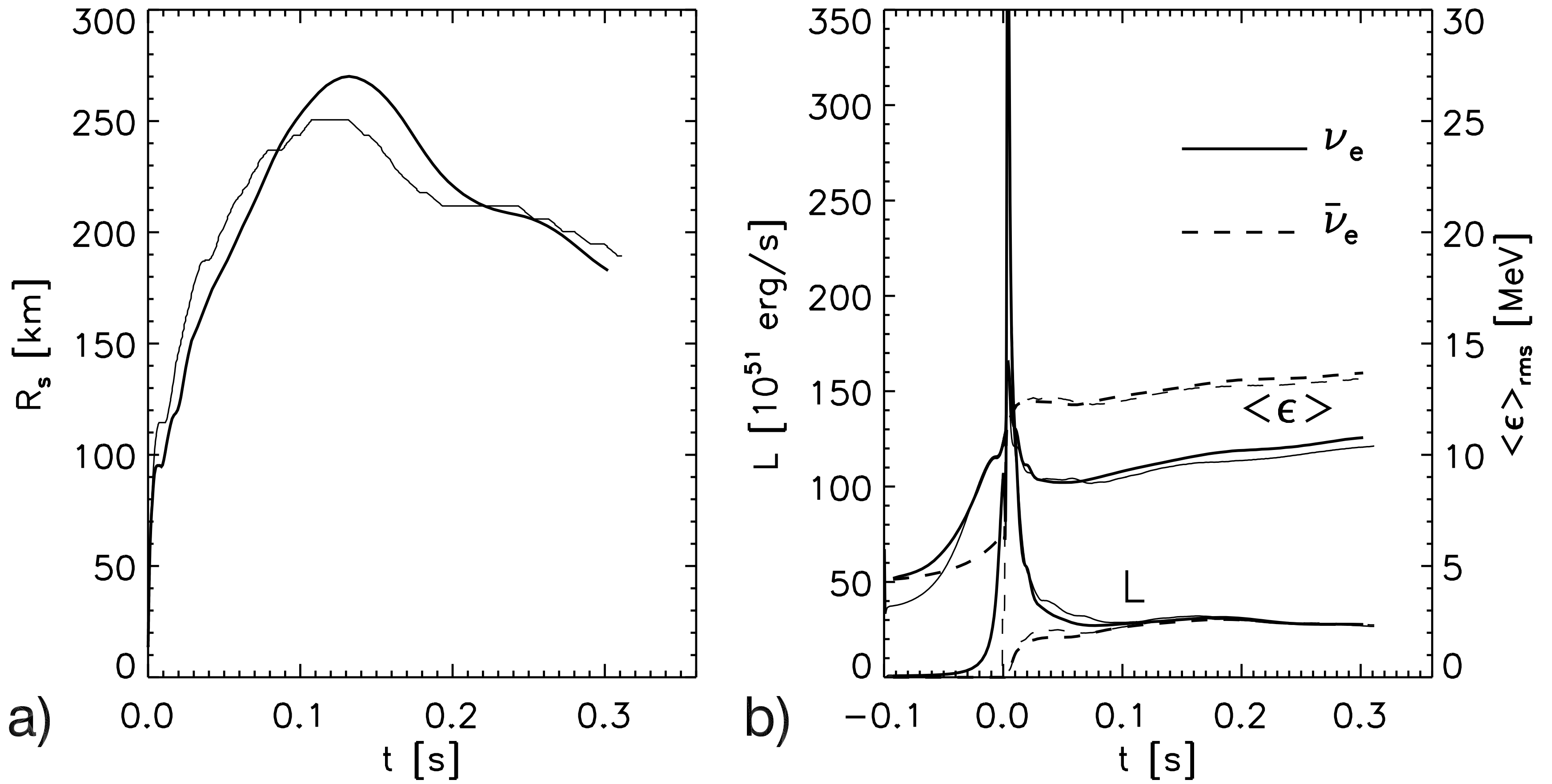

FIG. 5.—(*a*) Shock position as a function of time for model N13. The shock in VERTEX (*thin line*) propagates initially faster and nicely converges after its maximum expansion to the position of the shock in AGILE-BOLTZTRAN (*thick line*). (*b*) Neutrino luminosities and rms energies for model N13 are presented as functions of time. The values are sampled at a radius of 500 km in the comoving frame. The solid lines belong to electron neutrinos and the dashed lines to electron antineutrinos. The line width distinguishes between the results from AGILE-BOLTZTRAN and VERTEX in the same way as in (*a*). The luminosity peaks are nearly identical; the rms energies have the tendency to be larger in AGILE-BOLTZTRAN.

Liebendörfer *et al.*, ApJ620(2005)840 Fig.5

- relatively good agreement among 1D simulations
- small multidimensional effects
- Emission of the other neutrino species is negligible during this phase
  $\Rightarrow$ neutrino oscillation effects prominent

2. accretion phase ($O(1)$sec) until the core explosion or BH formation
shock wave propagation, stall, revival (leading to explosion) or BH formation
All types of neutrinos are in equilibrium inside the neutrinosphere and diffuse out from the hot accreted mantle.

Light ONe core + CO shell($1.38M_\odot$): weak explosion ($O(10^{50})$erg)
ν-heating + nuclear reaction $\Rightarrow$ weak explosion (Progenitor: Nomoto 8-10$M_\odot$)

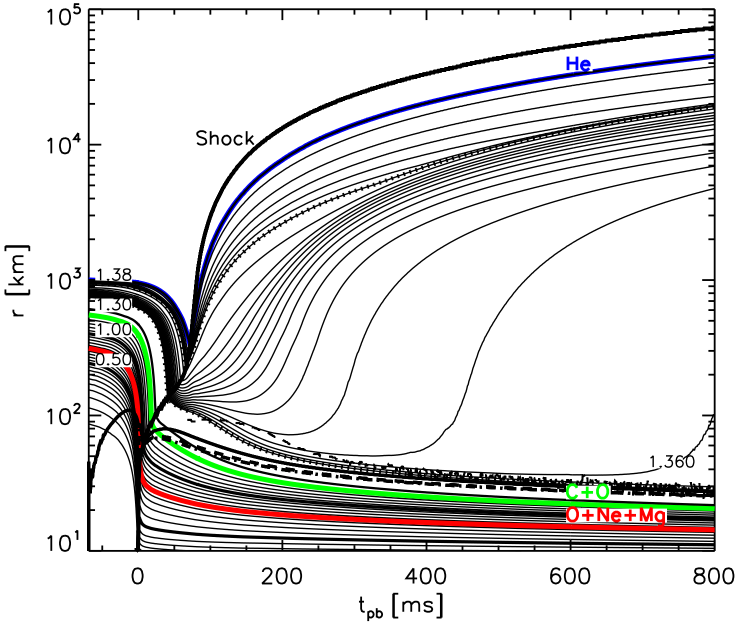

Fig. 1. Mass trajectories for the simulation with the W&H EoS as a function of post-bounce time (t_{pb}). Also plotted: shock position (thick solid line starting at time zero and rising to the upper right corner), gain radius (thin dashed line), and neutrinospheres (ν_e: thick solid; $\bar{\nu}_e$: thick dashed; ν_μ, $\bar{\nu}_\mu$, ν_τ, $\bar{\nu}_\tau$: thick dash-dotted). In addition, the composition interfaces are plotted with different bold, labelled lines: the inner boundaries of the O-Ne-Mg layer at ~0.77 $M_\odot$, of the C-O layer at ~1.26 $M_\odot$, and of the He layer at 1.3769 $M_\odot$. The two dotted lines represent the mass shells where the mass spacing between the plotted trajectories changes. An equidistant spacing of $5\times10^{-2}M_\odot$ was chosen up to $1.3579M_\odot$, between that value and $1.3765M_\odot$ it was $1.3\times10^{-3}M_\odot$, and $8\times10^{-5}M_\odot$ outside.

Kitaura *et al.*, AAp 450(2006)345

Crab pulsar is thought to be formed in this kind of explosion.

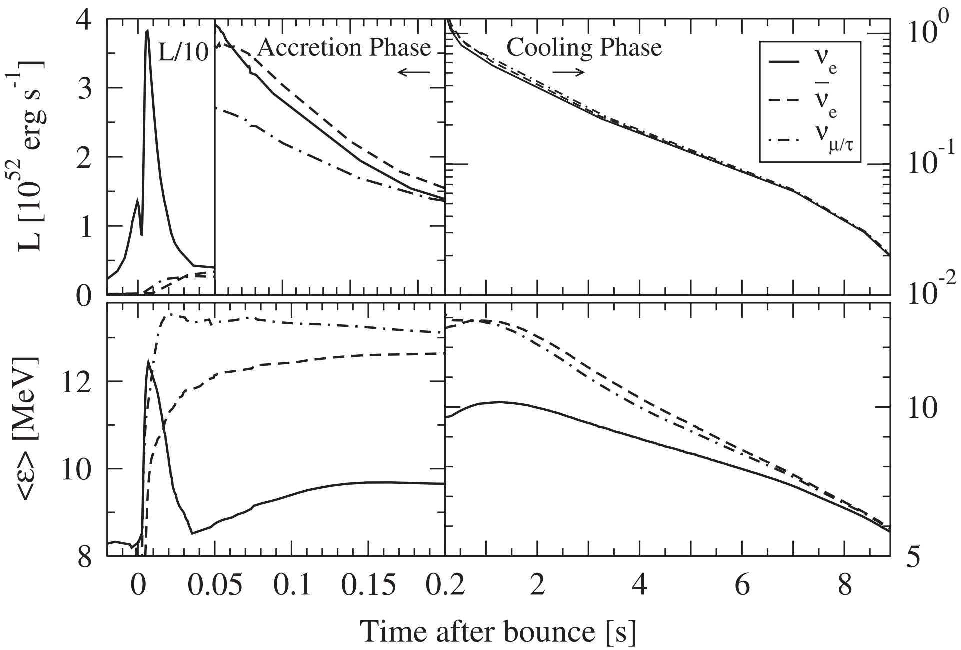

Neutrino luminosities and average energies at infinity for $8.8M_\odot$ progenitor.

L. Hüdepohl *et al.*, PRL104 (2010) 251101

Modern simulations with GR 1D Boltzmann ν-transfer

canonical models: no explosion

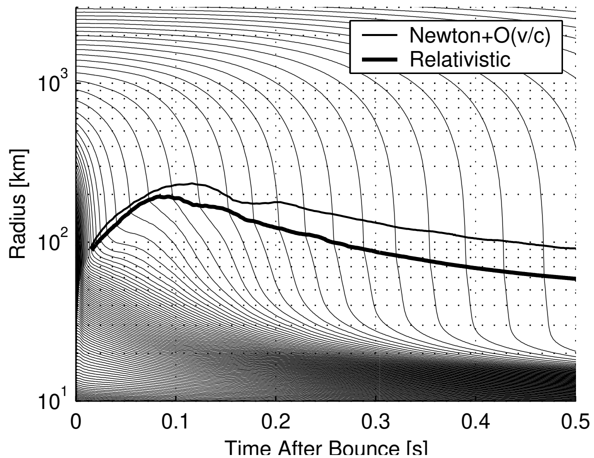

Liebendörfer *et al.*, Phys.Rev. D63 (2001) 103004

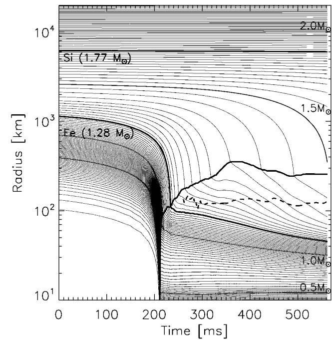

FIG. 1.—Trajectories of selected mass shells vs. time from the start of the simulation. The shells are equidistantly spaced in steps of 0.02 $M_\odot$, and the trajectories of the outer boundaries of the iron core (at 1.28 $M_\odot$) and of the silicon shell (at 1.77 $M_\odot$) are indicated by thick lines. The shock is formed at 211 ms. Its position is also marked by a thick line. The dashed curve shows the position of the gain radius.

Rampp *et al.*, ApJ 539 (2000) L33 Fig.1

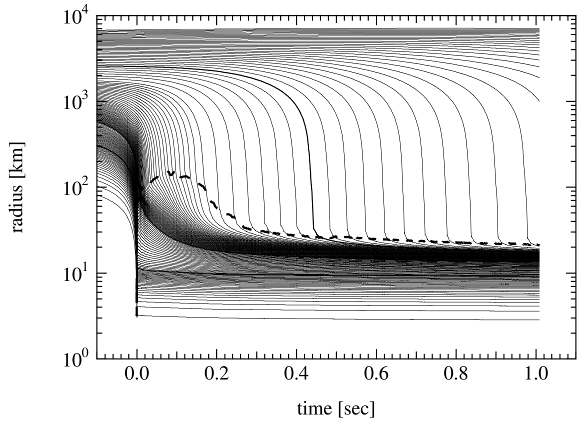

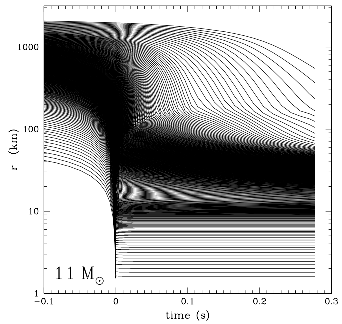

FIG. 5.—Radial position (in km) of selected mass shells as a function of time in our fiducial 11 $M_\odot$ model.

Thompson *et al.*, ApJ 592 (2003) 434 Fig.5

$15M_\odot$, Shen EOS, Sumiyoshi *et al.*, 2005.

Neutrino Interactions (minimal standard: Bruenn'85)

$e^-p \longleftrightarrow \nu_e n$	$e^+n \longleftrightarrow \bar{\nu}_e p$	$e^-A \longrightarrow \nu_e A'$	$e^+A \longrightarrow \bar{\nu}_e A'$
$e^-e^+ \longleftrightarrow \nu\bar{\nu}$	plasmon $\longleftrightarrow \nu\bar{\nu}$	$NN \longrightarrow NN\nu\bar{\nu}$	$\nu_e\bar{\nu}_e \longleftrightarrow \nu_x\bar{\nu}_x$
$\nu N \longrightarrow \nu N$	$\nu A \longrightarrow \nu A$	$\nu e^\pm \longrightarrow \nu e^\pm$	$\nu\nu' \longrightarrow \nu\nu'$

e-cap, ν emission, photodissociation $\rightarrow$ shock wave weakens and stalls

SN1987A
aspherical feature

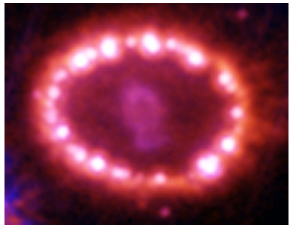

HST image of SN1987A
on 1994.2 and 2003.11.28

Multidimensional effects to revive the shock wave

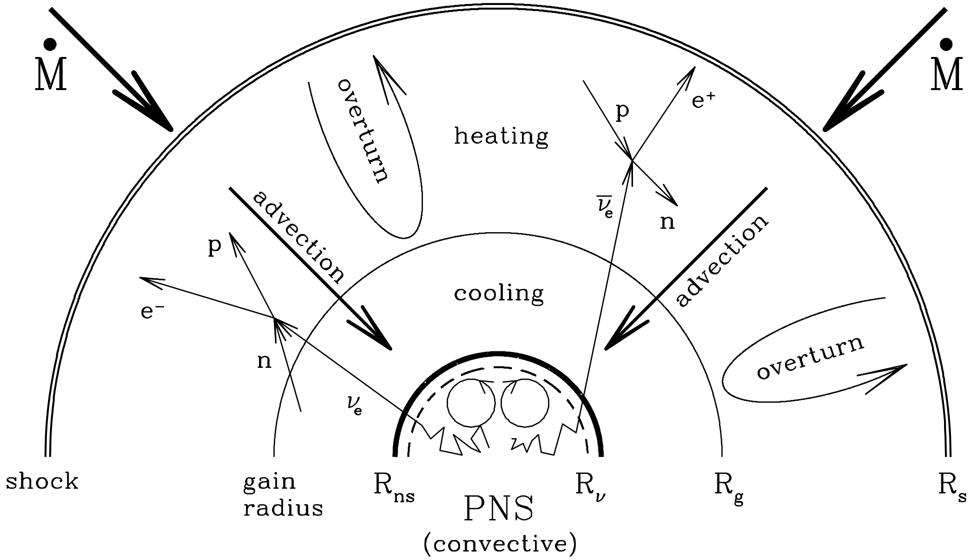

(Janka 1997)

gain radius: net neutrino heating rate=0
(heating $(T^6_{\nu\mathrm{sp}}\frac{R^2_{\nu\mathrm{sp}}}{r^2})$ = cooling $(T_{\mathrm{matter}}(r)^6)$)

- PNS convection inside neutrinosphere
  increase neutrino luminosity → more heating
- instability between shock front and neutrinosphere
  - neutrino convection: bottom of gain region is heated by ν's
  - SASI (Standing Accretion Shock Instability)
    accreting matter stay long in gain region: Δt(gain region) ↗
    ΔQ(ν heating) $\sim \dot{Q}\Delta t$(gain region) ↗: $\tau_{\mathrm{heating}} < \tau_{\mathrm{advection}} \Rightarrow$ Exp.

2D/3D simulations with various approximations (GR, neutrino transfer)

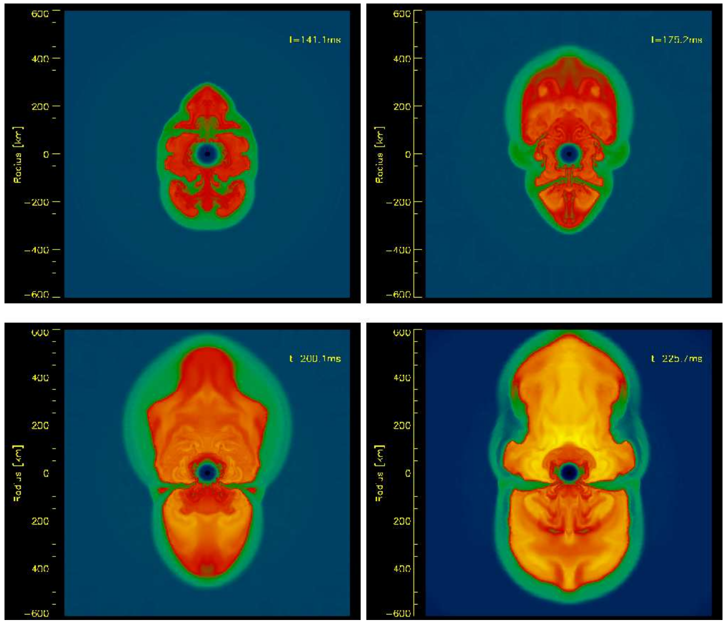

entropy profiles: Janka *et al.*,2007.

SASI: the shock front sloshes upward/downward

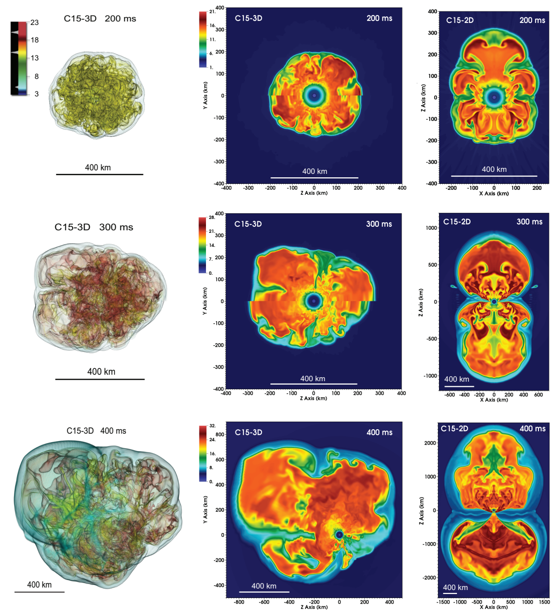

Figure 4. Specific entropy (k_B baryon^{-1}) at 200, 300, and 400 ms with 400-km scale bars in each panel. Column a (left): Volume rendering for C15-3D using a fixed transfer function, highlighting rising plumes. Column b (center): Polar slice through C15-3D, aligned with Column a. In upper two panels (200 and 300 ms), the 180° ϕ-shift between upper and lower halves is exaggerated by the 8.5° zone at the pole. 400-ms panel shows effect of transition to ϕ-averaging at pole. Column c (right): Entropy in a polar slice through C15-2D with color scale matching Column b at each epoch. Animated version of Column c available at ChimeraSN.org.

Lentz *et al.*, 2015

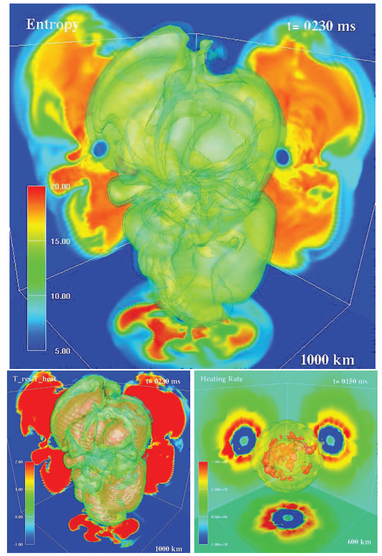

FIG. 1.— Three dimensional plots of entropy per baryon (top panel), $\tau_{\rm res}/\tau_{\rm heat}$ (bottom left panel) that is the ratio of the residency to the neutrino heating timescale (see the text for details), and the net neutrino heating rate (bottom right panel, in unit of erg cm^{-3} s^{-1}) for three snapshots (top and bottom left: $t = 230$ ms, and bottom right: $t = 150$ ms measured after bounce ($t \equiv 0$) of our model 3D-H-1). The contours on the cross sections in the $x = 0$ (back right), $y = 0$ (back bottom), and $z = 0$ (back left) planes are, respectively, projected on the sidewalls of the graphs. For each snapshot, the length of white line is indicated at right bottom text.

Takiwaki *et al.*, 2013

2D/3D simulations → explosions
(but many models: $E_{\rm exp} \lesssim$ obs. $O(10^{51})$erg)

key physics is still unclear

Neutrino Heating, Standing Accretion Shock Instability (SASI), Convection, Rotation, Magnetic Field, Acoustic Wave, asphericity in Si/O layer ?
+ sophistication of EOS and neutrino interaction rates
GR 3D+3D $f_\nu(t, x, y, z, p_{\nu x}, p_{\nu y}, p_{\nu z})$ simulations for long timescale are required.

Neutrinos from 3D simulations
(results depend on progenitor, EOS, dimensionality, numerical scheme)

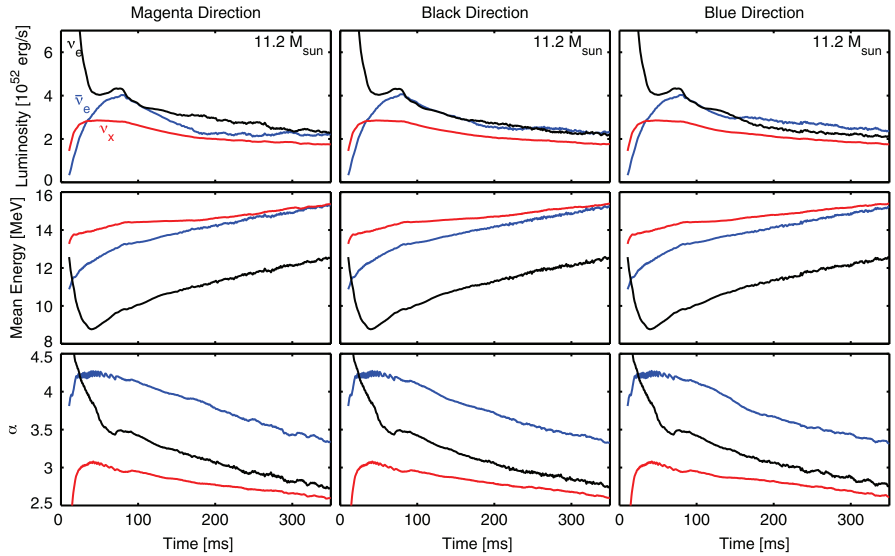

FIG. 5 (color online). Evolution of neutrino flux properties for the $11.2 M_\odot$ progenitor as seen from a distant observer. For ν_e, $\bar{\nu}_e$, and ν_x we show the luminosity, average energy, and shape parameter α. The Magenta and Blue directions are opposite along the LESA axis, corresponding to the magenta and blue curves in Fig. 4, whereas the Black direction is on the LESA equator (black in Fig. 4).

$11.2 M_\odot$

Convection develops and SASI does not grow.

Shock wave revives before the SASI grows.

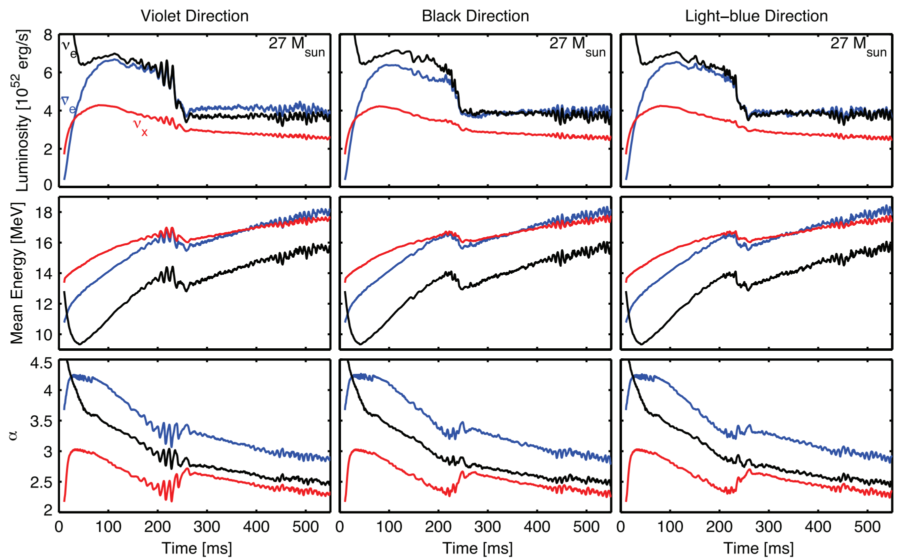

FIG. 6 (color online). Same as Fig. 5, but for the $27 M_\odot$ progenitor. The Violet, Black, and Light Blue directions here correspond to the curves of the same color in Fig. 7 that were chosen to show large and small SASI amplitudes, respectively.

$27 M_\odot$

SASI grows slowly.

$\Rightarrow L_\nu(t)$ oscillates with SASI frequency.

2D model explodes, but
3D model does not yet.

Tamborra *et al.*, 2014

Systemitics?

Structure of progenitors does not have monotonic relations to initial mass.

compactness parameter $\xi_M \equiv \frac{M/M_\odot}{r(M)/1000\,\mathrm{km}}$ (O'connor and Ott 2011)

progenitors with large ξ cannot explode due to dense surrounding of Fe core.

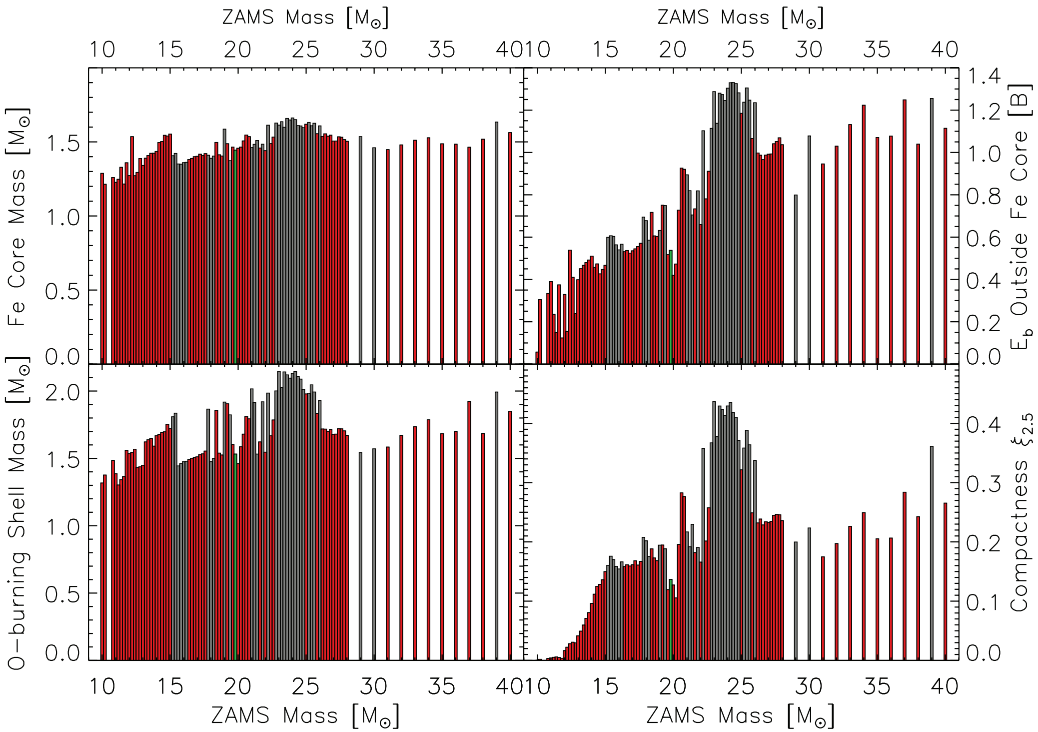

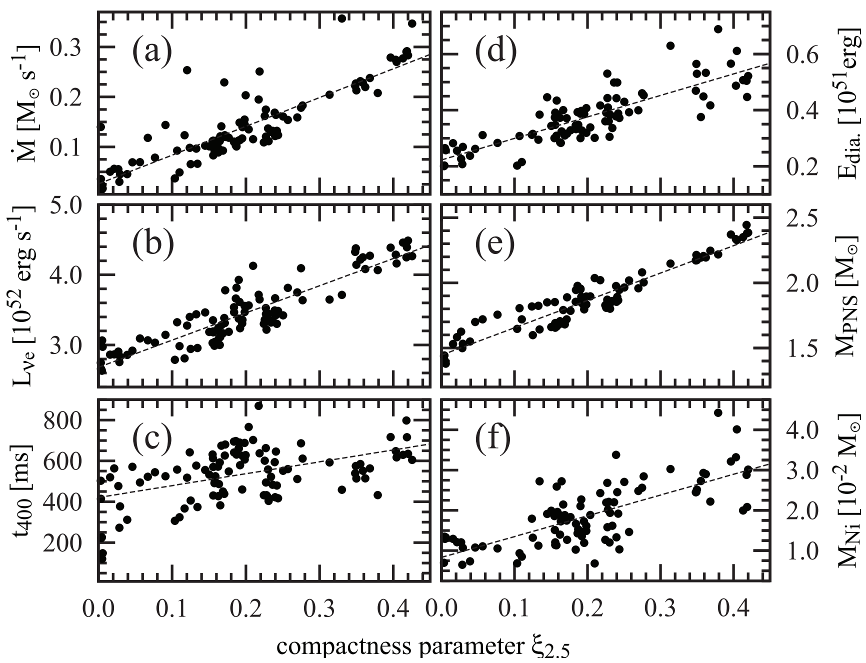

Ugliano *et al.*, 2012 and Nakamura *et al.*, 2015

other good parameters ? $M_4 \equiv M(s=4) \sim$ Si/O I/F,

$\mu_4 \equiv \frac{300\mathrm{km}}{r(M_4+0.3M_\odot)-r(s=4)} \propto \frac{dM}{dr}|_{s=4}$

full 3D+3D neutrino transfer code ($f_\nu(t, r, \theta, \phi, p_\nu, \theta_\nu, \phi_\nu)$) by Yamada group

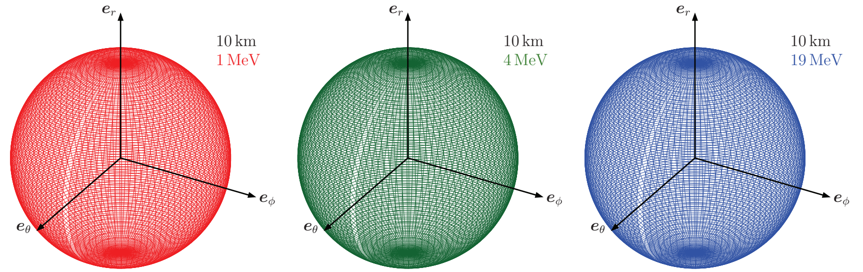

Figure 4. Angular distributions in momentum space of the electron-type neutrino at 12 ms after bounce in the laboratory frame. The spatial point is $r = 10$ km in the optically thick region on the equator. Each panel represents different neutrino energies measured in the laboratory frame: red–1 MeV, green–4 MeV, blue–19 MeV. Arrows with $\boldsymbol{e}_r$, $\boldsymbol{e}_\theta$, and $\boldsymbol{e}_\phi$ represent the spatial bases of the tetrad (equations (2–4)). All distributions are normalized so that the maximum value is the same, say, unity. In order to make the surfaces smooth, angular interpolation is applied.

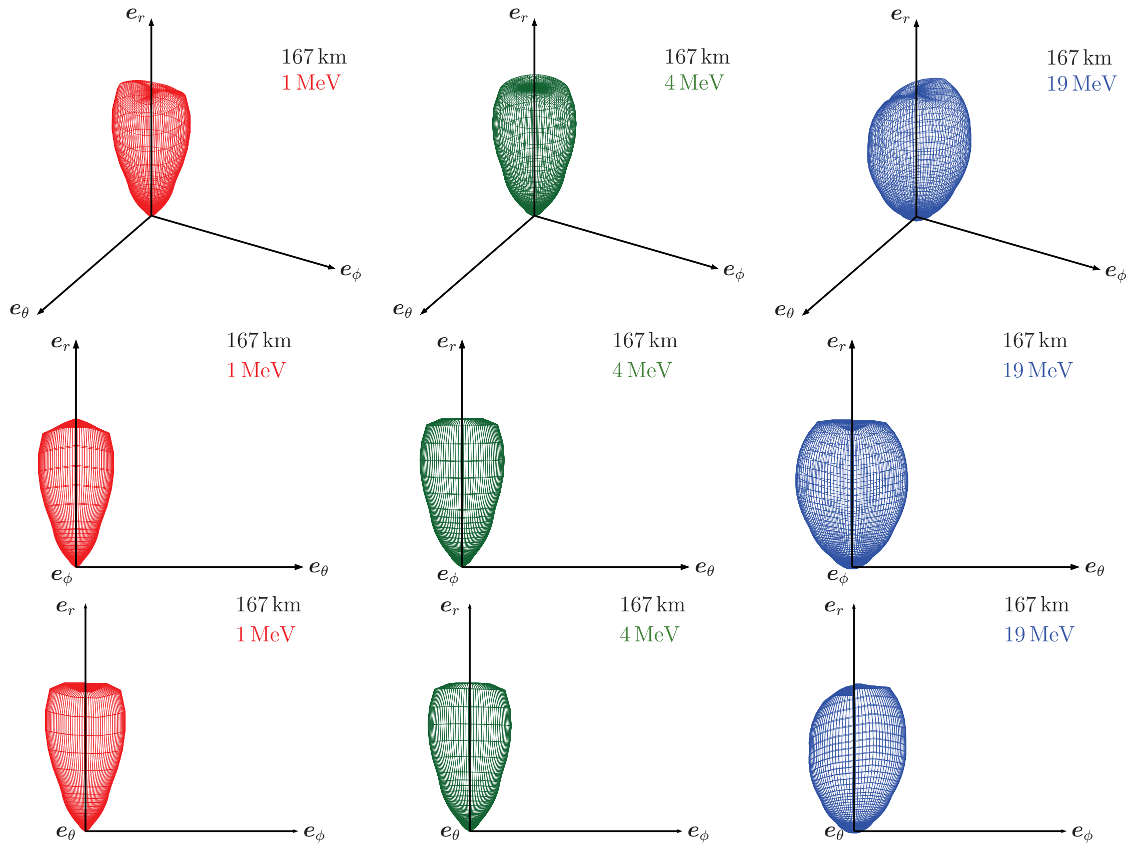

Figure 6. The same as figure 5 except that the spatial point is $r = 167$ km in the optically thin region.

In the central region, neutrino distribution is isotropic.

Outer regions: asymmetric distribution depending on neutrino energy.

Harada *et al.*, 2019

accretion phase: general feature

- thermal neutrino emission (all species)
- hierarchy of mean energy

cross section	σ_{ν_e}	$>$	$\sigma_{\bar{\nu}_e}$	$>$	σ_{ν_x}
$\rho_{\rm neutrinosphere}$	ρ_{ν_e}	$<$	$\rho_{\bar{\nu}_e}$	$<$	ρ_{ν_x}
$R_{\rm neutrinosphere}$	R_{ν_e}	$>$	$R_{\bar{\nu}_e}$	$>$	R_{ν_x}
$T_{\rm neutrinosphere}$	T_{ν_e}	$<$	$T_{\bar{\nu}_e}$	$<$	T_{ν_x}
average energy	$\langle\omega_{\nu_e}\rangle$	$<$	$\langle\omega_{\bar{\nu}_e}\rangle$	$<$	$\langle\omega_{\nu_x}\rangle$

- $L_\nu \propto \dot{M}$: indication of shock revival time

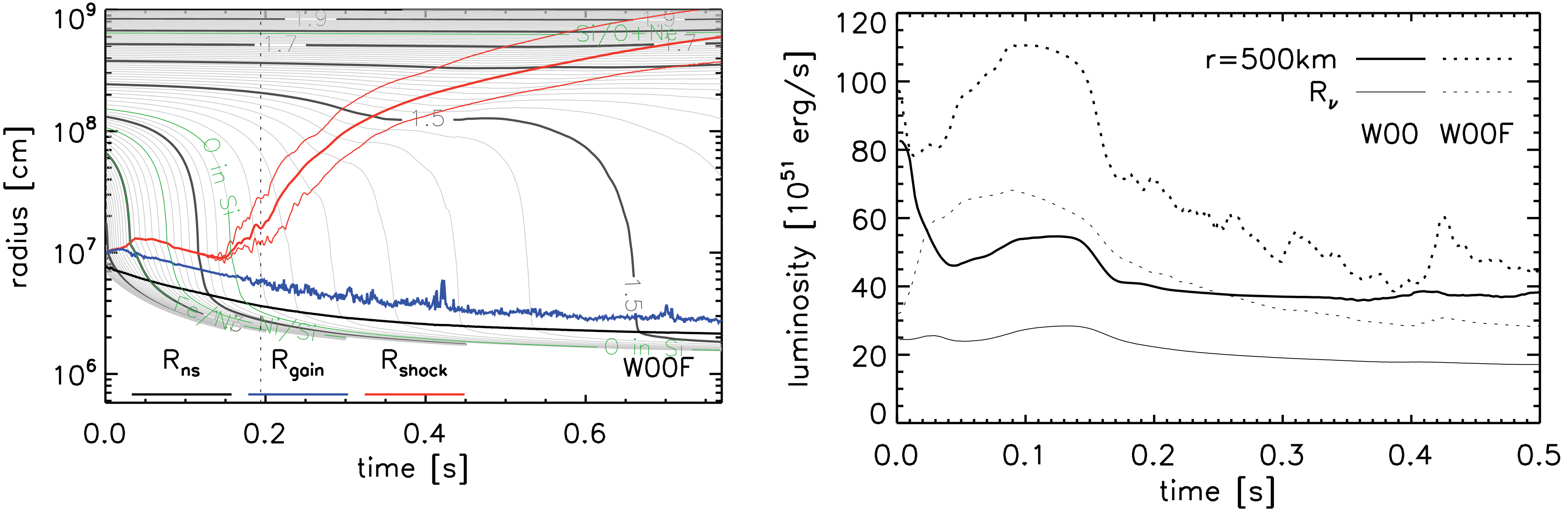

2D explosion by Scheck *et al.*, 2008: thick dotted line is $L_\nu(t)$ in the right panel.

Failed supernovae (Black Hole formation)

1D implicit GR hydrodynamics + Boltzmann ν transfer code

Sumiyoshi, Yamada, Suzuki, Chiba PRL97(2006) 091101

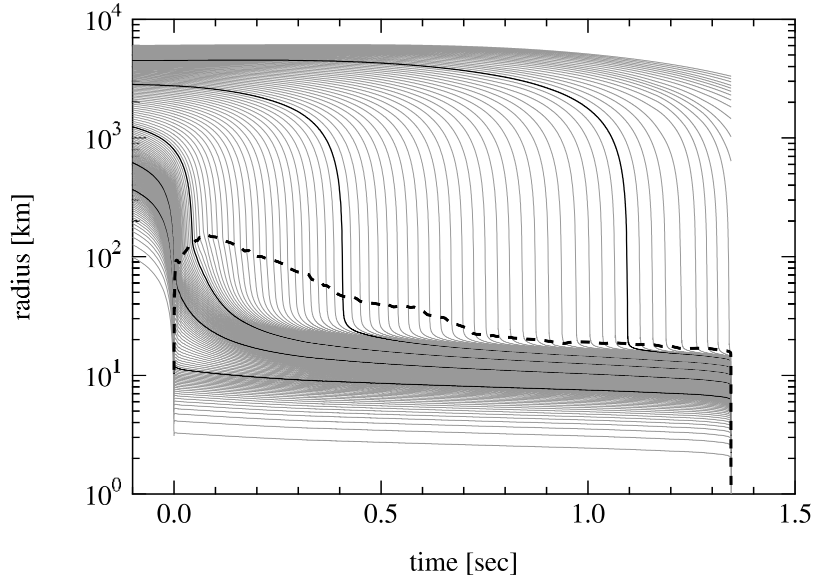

FIG. 1.—Radial trajectories of mass elements of the core of a 40 $M_\odot$ star as a function of time after bounce in the SH model. The location of the shock wave is shown by a thick dashed line.

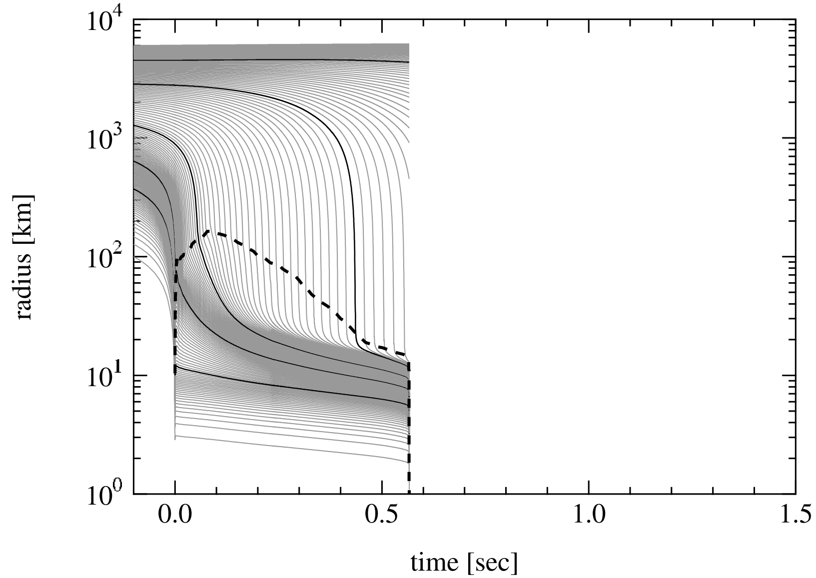

FIG. 2.—Radial trajectories of mass elements of the core of a 40 $M_\odot$ star as a function of time after bounce in the LS model. The location of the shock wave is shown by a thick dashed line.

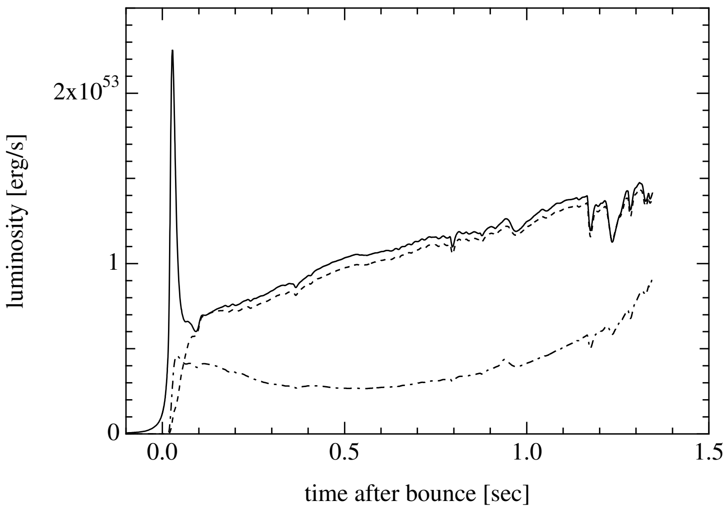

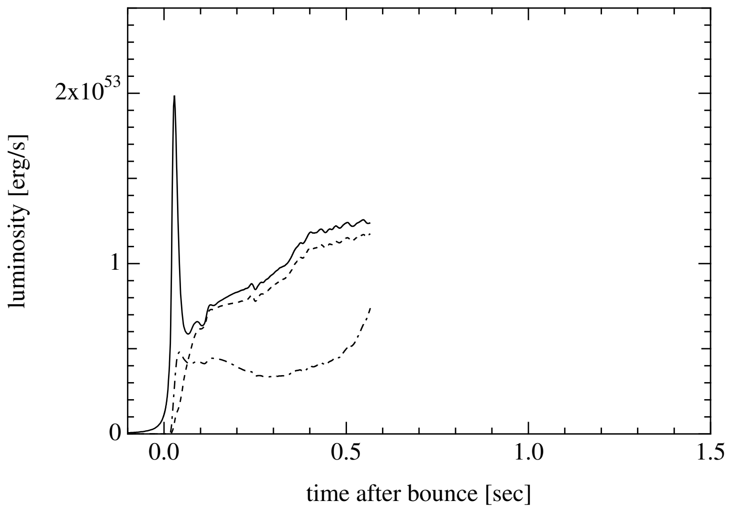

L_ν increases due to matter accretion

$\nu_x < \nu_e, \bar{\nu}_e$ from accreted matter

Burst duration time strongly depends on EOS!

Progenitor $40M_\odot$, left: Shen EOS (stiffer), right: Lattimer-Swesty EOS 180 (softer)

3. cooling phase: Proto Neutron Star (PNS) cooling ($O(10-100)$sec)

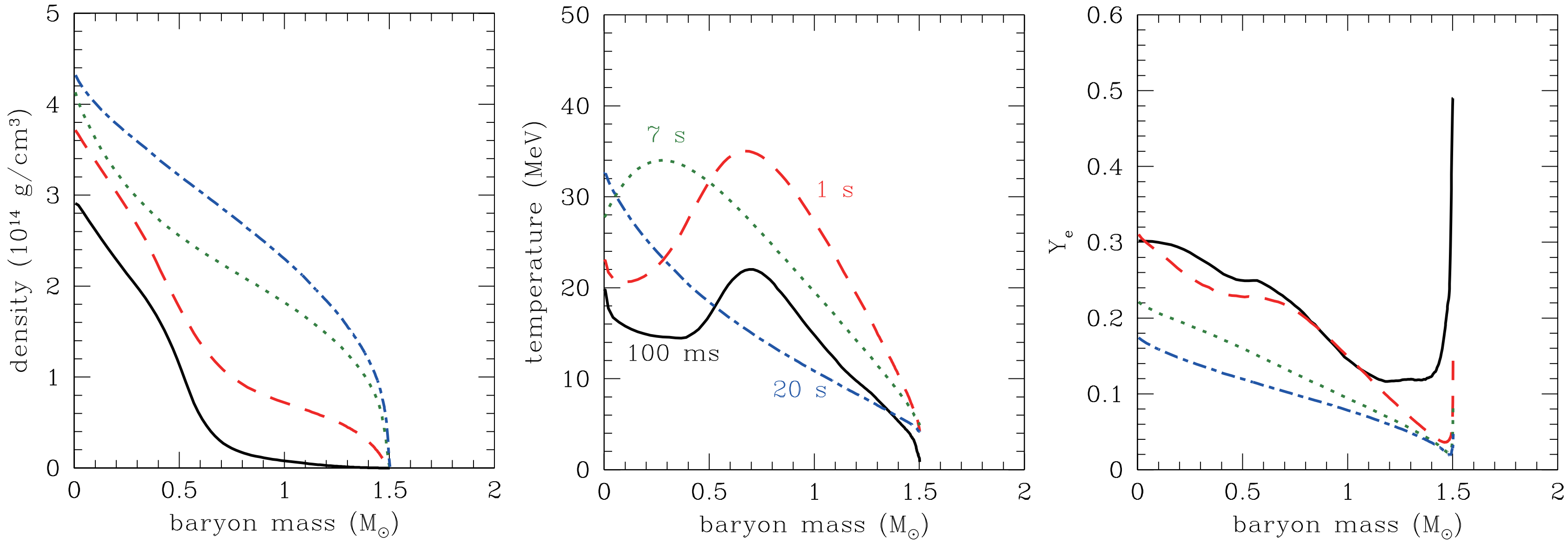

Figure 8. Evolutions of the density, temperature, and electron fraction profiles by the simulation of proto-neutron star cooling for the model with initial mass $M_{\rm init} = 13\,M_\odot$, metallicity $Z = 0.02$, and shock revival time $t_{\rm revive} = 100$ ms. In all panels, solid, dashed, dotted, and dot-dashed lines correspond to the times at 100 ms, 1 s, 7 s, and 20 s after the bounce, respectively.

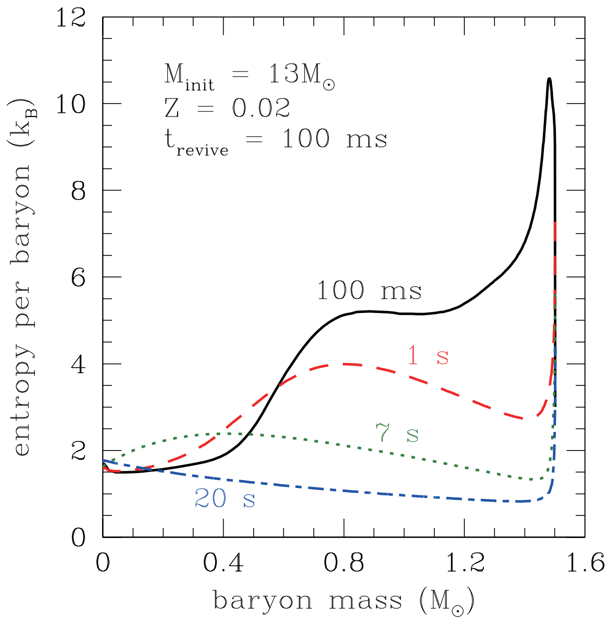

Figure 9. Snapshots of entropy profiles for the model with initial mass $M_{\rm init} = 13\,M_\odot$, metallicity $Z = 0.02$ and shock revival time $t_{\rm revive} = 100$ ms. The line notations are the same as those in Figure 8.

Nakazato *et al.*, ApJS205 (2013) 2

- cooling of mantle, contraction $\to T_{\rm mantle} \nearrow$
- $\bar{\nu}_{\rm e}$ and ν_x transport energy to the central region $\to S_{\rm center}, T_{\rm center} \nearrow$
- neutronization $\to$ ν-less β-equilibrium
- cooling of the whole neutron star

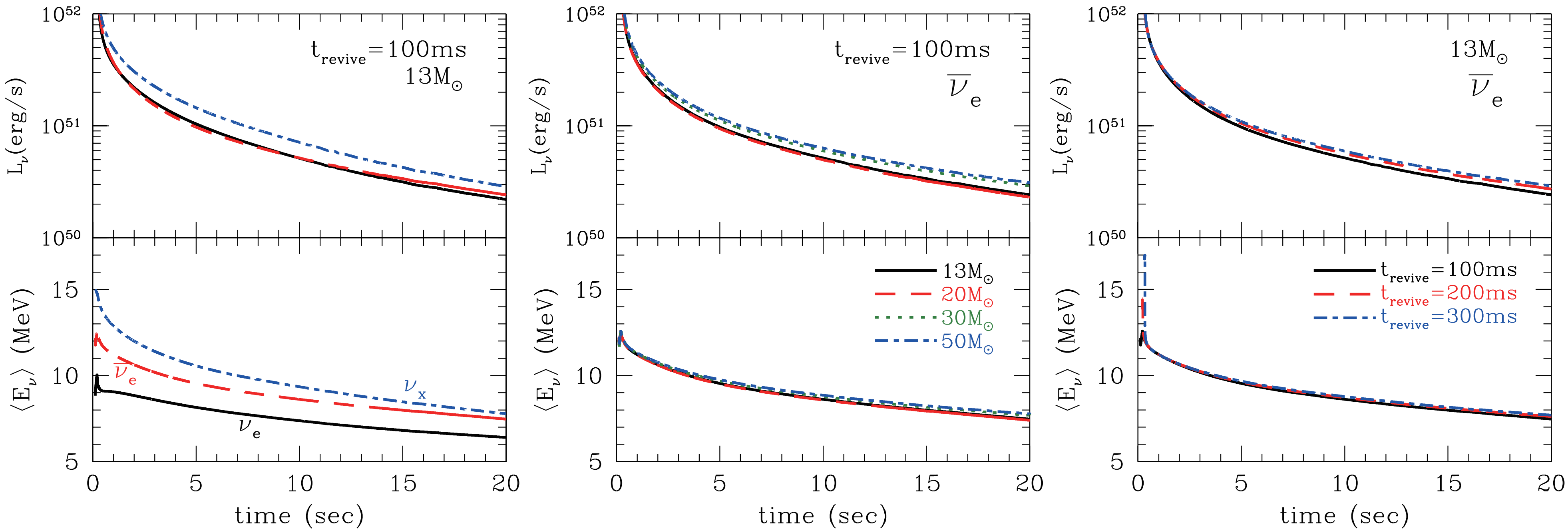

Figure 13. Same as Figure 12 but from the PNSC simulations. In the left panel, signals of ν_e (solid lines), $\bar{\nu}_e$ (dashed lines), and ν_x (dot-dashed lines) are shown for the model with $(M_{\rm init}, Z, t_{\rm revive}) = (13\,M_\odot, 0.02, 100\text{ ms})$. In the central panel, $\bar{\nu}_e$ signals are shown for the models with $(Z, t_{\rm revive}) = (0.02, 100\text{ ms})$ and $M_{\rm init} = 13\,M_\odot$ (solid lines), $20\,M_\odot$ (dashed lines), $30\,M_\odot$ (dotted lines), and $50\,M_\odot$ (dot-dashed lines). In the right panel, $\bar{\nu}_e$ signals are shown for the models with $(M_{\rm init}, Z) = (13\,M_\odot, 0.02)$ and $t_{\rm revive} = 100$ ms (solid lines), 200 ms (dashed lines), and 300 ms (dot-dashed lines).

Nakazato *et al.*, 2013, 1D simulations

- nearly spherical again
- differences among the neutrino species become small

neutronization and cooling:

$n(\mathrm{e}^+)\searrow$, Degeneracy of e^-, p, n$\nearrow$ (Pauli Blocking)

$\Rightarrow$ suppress charged current interactions (origin of differences among ν species)

$\mathrm{pe}^- \to \nu_\mathrm{e}\mathrm{n}$, $\mathrm{ne}^+ \to \bar{\nu}_\mathrm{e}\mathrm{p}$

Summary 1

- Collapse and bounce phase: neutronization burst of ν_{e}
  uncertainty is relatively small
  because the multidimensional effects do not have enough time to grow substantially and because the uncertainty of nuclear EOS is small around the nuclear density (density at which the core bounce occurs).
- Accretion and core explosion phase:
  state-of-the-art 1D simulation: light core explodes weakly, canonical cores do not explode.
  2D/3D simulations: explosion mechanism is still unknown, neutrinos will give us information.
  Instability like SASI might cause time variation of neutrino luminosity.
  At the shock revival, matter accretion onto inner core ceases and the neutrino luminosity drops.
  3D simulations with full general relativity and 3D neutrino transfer are required.
- Cooling phase: after the core explosion (cooling stage of the new-born protoneutron star), differences among neutrino species are small.

Our SN neutrino database (`http://asphwww.ph.noda.tus.ac.jp/snn/`)

Nakazato *et al.*, ApJS205 (2013) 2

- several progenitor models
  Initial stellar mass and metallicity: $M = 13, 20, 30, 50 M_\odot$, $Z = Z_\odot, 0.2Z_\odot$
  evolution of neutrino energy spectra for various progenitor models are provided as numerical data.
- Users can choose a parameter (shock revival time) which is introduced in order to incorporate multidimensional effects into our 1D simulations.
  Neutrino flux from unexploded dynamical simulations and that from cooling simulations of proto neutron star stripped of the ejecta are interpolated by use of the shock revival time.

Basic Idea

Neutrino luminosities from unexploded 1D simulations correspond to the upper bound because the multidimensional effects helping the explosion would prevent the matter accretion onto the SN core ($\dot{M} \propto L_\nu$).
On the other hand, the neutrino luminosities from protoneutron star cooling simulations correspond to the lower bound because the overlying matter is stripped and no further accretion occurs in the simulations.
We interpolated the two limits to mimic the actual neutrino luminosities with a model parameter corresponding to the shock revival time after which the matter accretion would cease.

Dynamical Phase: 1D simulations (not explode)

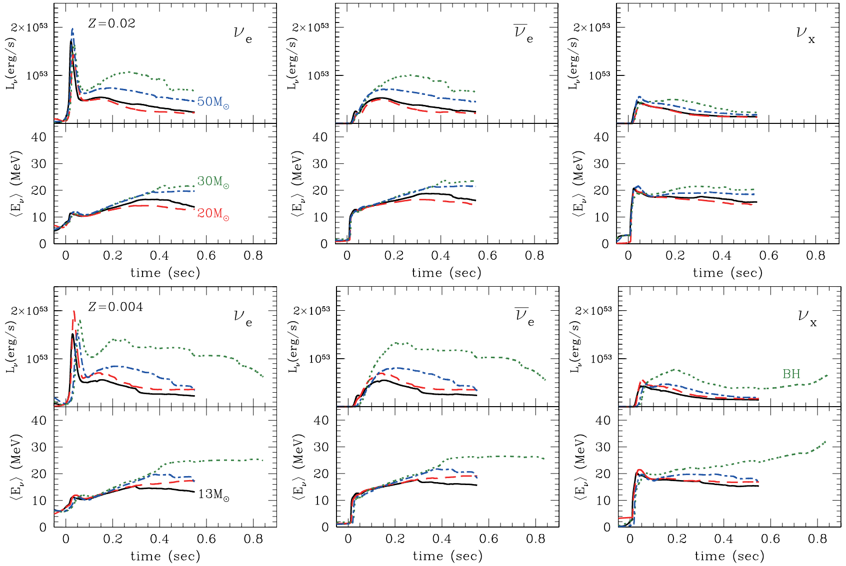

Figure 12. Luminosities (upper plots) and average energies (lower plots) of the emitted neutrinos as a function of time after the bounce from the νRHD simulations. The panels correspond, from left to right, to ν_e, $\bar{\nu}_e$, and ν_x ($= \nu_\mu, \nu_\tau, \bar{\nu}_\mu, \bar{\nu}_\tau$). The results for the models with metallicity $Z = 0.02$ are shown in the top panels, and those for the models with $Z = 0.004$ are shown in the bottom panels. In all panels, solid, dashed, dotted, and dot-dashed lines correspond to the models with initial mass $M_{\rm init} = 13\,M_\odot$, $20\,M_\odot$, $30\,M_\odot$, and $50\,M_\odot$, respectively. "BH" means a black-hole-forming model with $M_{\rm init} = 30\,M_\odot$ and $Z = 0.004$; its end point corresponds to the moment of black hole formation.

Proto Neutron Star Cooling Phase

initial models = central part inside the shock front at assumed shock revival time $t_{\rm rev}$ in dynamical models (assuming that successful explosion expels overlying matter)

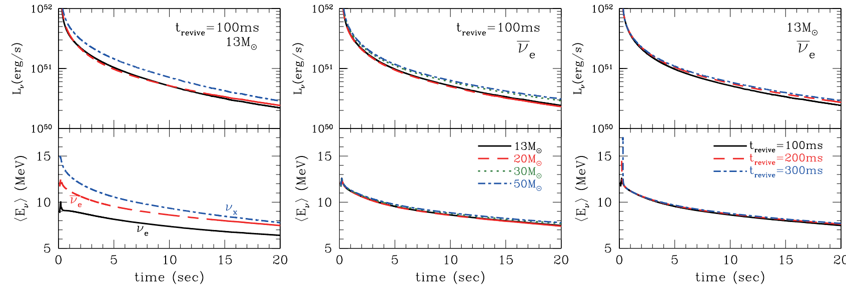

Figure 13. Same as Figure 12 but from the PNSC simulations. In the left panel, signals of ν_e (solid lines), $\bar{\nu}_e$ (dashed lines), and ν_x (dot-dashed lines) are shown for the model with $(M_{\rm init}, Z, t_{\rm revive}) = (13\,M_\odot, 0.02, 100\ {\rm ms})$. In the central panel, $\bar{\nu}_e$ signals are shown for the models with $(Z, t_{\rm revive}) = (0.02, 100\ {\rm ms})$ and $M_{\rm init} = 13\,M_\odot$ (solid lines), $20\,M_\odot$ (dashed lines), $30\,M_\odot$ (dotted lines), and $50\,M_\odot$ (dot-dashed lines). In the right panel, $\bar{\nu}_e$ signals are shown for the models with $(M_{\rm init}, Z) = (13\,M_\odot, 0.02)$ and $t_{\rm revive} = 100$ ms (solid lines), 200 ms (dashed lines), and 300 ms (dot-dashed lines).

$$F_{\nu_i}(E,t) = F_{\nu_i}^{\rm acc}(E,t) + F_{\nu_i}^{\rm PNSC}(E,t) \sim f(t) F_{\nu_i}^{\rm dyn}(E,t) + (1-f(t)) F_{\nu_i}^{\rm PNSC}(E,t)$$

$$F_{\nu_i}^{\rm acc}({\rm explosion}) = f(t) F_{\nu_i}^{\rm acc,max} = f(t)(F_{\nu_i}^{\rm dyn}({\rm no\ explosion}) - F_{\nu_i}^{\rm PNSC}({\rm no\ accretion}))$$

$$f(t) \equiv \begin{cases} 1 & t < t_{\rm rev} + t_{\rm shift} \\ \exp\left(-\frac{t-(t_{\rm rev}+t_{\rm shift})}{\tau_{\rm decay}}\right) & t > t_{\rm rev} + t_{\rm shift} \end{cases}$$

model parameter: shock revival time ($t_{\rm rev}$)

explosion with effective ν convection $\rightarrow$ small $t_{\rm rev}$

if SASI is essential $\rightarrow$ large $t_{\rm rev}$ (larger than growth time of SASI)

SN neutrino database (`http://asphwww.ph.noda.tus.ac.jp/snn/`)

Nakazato *et al.*, ApJS205 (2013) 2

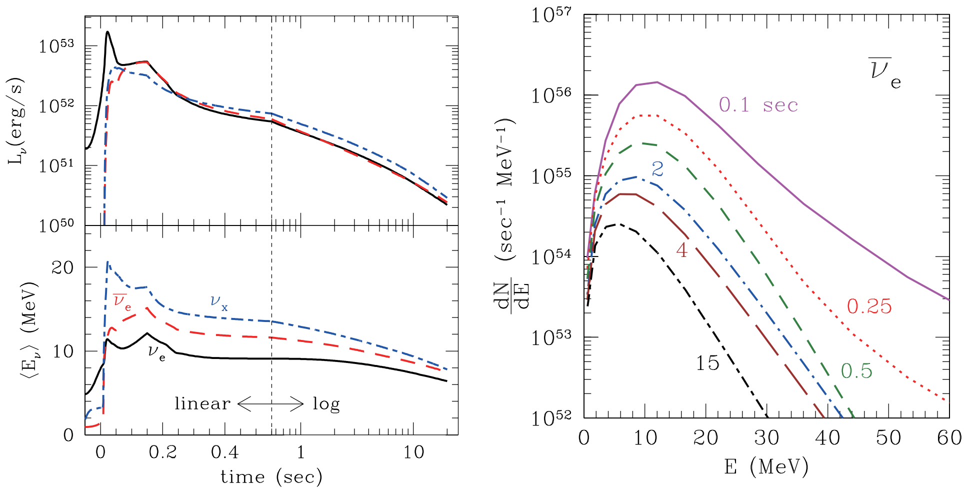

Figure 14. Time evolution of neutrino luminosity and average energy (left) and number spectrum of $\bar{\nu}_e$ (right) from νRHD and PNSC simulations with the interpolation (13) for the model with $(M_{\rm init}, Z, t_{\rm revive}) = (13\,M_\odot, 0.02, 100\text{ ms})$. In the left panel, solid, dashed, and dot-dashed lines represent ν_e, $\bar{\nu}_e$, and ν_x (dot-dashed lines), respectively. In the right panel, the lines correspond, from top to bottom, to 0.1, 0.25, 0.5, 2, 4, and 15 s after the bounce.

Table 1
Key Parameters for All Models

Z	$M_{\rm init}$ ($M_\odot$)	$M_{\rm tot}$ ($M_\odot$)	$M_{\rm He}$ ($M_\odot$)	$M_{\rm CO}$ ($M_\odot$)	$M_{\rm core}$ ($M_\odot$)	$t_{\rm revive}$ (ms)	$M_{b,\rm NS}$ ($M_\odot$)	$M_{g,\rm NS}$ ($M_\odot$)	$\langle E_{\nu_e}\rangle$ (MeV)	$\langle E_{\bar{\nu}_e}\rangle$ (MeV)	$\langle E_{\nu_x}\rangle$ (MeV)	$E_{\nu_e,\rm tot}$ (10^{52} erg)	$E_{\bar{\nu}_e,\rm tot}$ (10^{52} erg)	$E_{\nu_x,\rm tot}$ (10^{52} erg)	$E_{\nu_{\rm all},\rm tot}$ (10^{53} erg)
0.02	13	12.3	3.36	1.97	1.55	100	1.50	1.39	9.08	10.8	11.9	3.15	2.68	3.19	1.86
						200	1.59	1.46	9.49	11.3	12.0	3.51	3.04	3.45	2.03
						300	1.64	1.50	9.91	11.7	12.1	3.83	3.33	3.59	2.15
	20	17.8	5.01	3.33	1.56	100	1.47	1.36	9.00	10.7	11.8	3.03	2.56	3.06	1.78
						200	1.54	1.42	9.32	11.1	11.9	3.30	2.82	3.27	1.92
						300	1.57	1.45	9.57	11.4	12.0	3.49	3.00	3.35	1.99
	30	23.8	8.54	7.10	2.06	100	1.62	1.49	9.32	11.1	12.1	3.77	3.23	3.72	2.19
						200	1.83	1.66	10.2	12.1	12.5	4.80	4.24	4.51	2.71
						300	1.98	1.78	11.1	13.0	12.8	5.76	5.16	4.99	3.09
	50	11.9	⋯	11.9	1.89	100	1.67	1.52	9.35	11.0	12.1	3.76	3.24	3.85	2.24
						200	1.79	1.63	9.98	11.7	12.3	4.39	3.85	4.28	2.53
						300	1.87	1.69	10.6	12.4	12.4	4.95	4.38	4.51	2.74
0.004	13	12.5	3.76	2.37	1.61	100	1.50	1.38	9.07	10.8	11.9	3.15	2.68	3.18	1.86
						200	1.58	1.45	9.47	11.3	12.0	3.51	3.03	3.45	2.03
						300	1.63	1.49	9.76	11.6	12.1	3.75	3.26	3.57	2.13
	20	18.9	5.18	3.43	1.76	100	1.63	1.49	9.28	11.0	12.0	3.68	3.12	3.72	2.17
						200	1.73	1.57	9.71	11.4	12.2	4.11	3.55	4.04	2.38
						300	1.77	1.61	10.1	11.9	12.3	4.43	3.84	4.20	2.51
	30	26.7	11.1	9.35	2.59	⋯	⋯	⋯	17.5	21.7	23.4	9.49	8.10	4.00	3.36
	50	16.8	⋯	16.8	1.95	100	1.67	1.52	9.10	10.9	12.0	3.83	3.19	3.81	2.23
						200	1.79	1.63	9.77	11.7	12.3	4.54	3.89	4.30	2.56
						300	1.91	1.72	10.5	12.5	12.5	5.20	4.51	4.61	2.81

Notes. $M_{\rm init}$ and Z are the initial mass and metallicity of progenitors, respectively. $M_{\rm tot}$, $M_{\rm He}$, and $M_{\rm CO}$ are the total progenitor mass, He core mass, and CO core mass when the collapse begins, respectively. Since models with $M_{\rm init} = 50\,M_\odot$ become Wolf–Rayet stars, $M_{\rm He}$ is not defined and $M_{\rm CO}$ equals $M_{\rm tot}$. $M_{\rm core}$ is a core mass defined as the region of oxygen depletion. $t_{\rm revive}$ is the shock revival time. $M_{b,\rm NS}$ and $M_{g,\rm NS}$ are the baryonic mass and gravitational mass of the remnant neutron states, respectively. The mean energy of emitted ν_i until 20 s after the bounce is denoted as $\langle E_{\nu_i}\rangle \equiv E_{\nu_i,\rm tot}/N_{\nu_i,\rm tot}$, where $E_{\nu_i,\rm tot}$ and $N_{\nu_i,\rm tot}$ are the total energy and number of neutrinos, respectively. ν_x stands for μ- and τ-neutrinos and their anti-particles: $E_{\nu_x} = E_{\nu_\mu} = E_{\bar{\nu}_\mu} = E_{\nu_\tau} = E_{\bar{\nu}_\tau}$. $E_{\nu_{\rm all},\rm tot}$ is the total of neutrino energy summed over all species. The model with $M_{\rm init} = 30\,M_\odot$ and $Z = 0.004$ is a black-hole-forming model, for which mean and total neutrino energies emitted up to the black hole formation are shown.

For the model with $M = 30 M_\odot, Z = 0.004$, BH will be formed because $M_{\rm Fe\,core} > 2.5 M_\odot$ is too heavy.

Supernova Relic Neutrino (SRN)
Diffuse Supernova Neutrino Background (DSNB)

- Core-Collapse Supernova Rate $R_{\rm CC}(z, M, Z)$
$\Leftarrow$ Star Formation Rate(SFR), Initial Mass Function (IMF), metallicity evolution (z: red-shift($\leftrightarrow$cosmic time), M: progenitor mass, Z: metallicity)
- Energy spectra from individual supernova $\frac{dN_\nu(E'_\nu, M, Z)}{dE'_\nu}$
using our SN neutrino database
- Cosmic expansion $\rightarrow$ red-shift of ν energy

$$\frac{dF_\nu(E_\nu, t_0)}{dE_\nu} = c\int_0^{t_0}\int_{M_{\rm min}}^{M_{\rm max}}\int_0^{Z_{\rm max}} \frac{d^2R_{\rm CC}(z, M, Z)}{dMdZ}dZdM\frac{dN_\nu(E'_\nu, M, Z)}{dE'_\nu}\frac{dE'_\nu}{dE_\nu}dt$$

$$dt = -\frac{dz}{(1+z)H(z)},\ H(z) = \sqrt{\Omega_m(1+z)^3 + \Omega_\Lambda}H_0,\ dE'_\nu = (1+z)dE_\nu$$

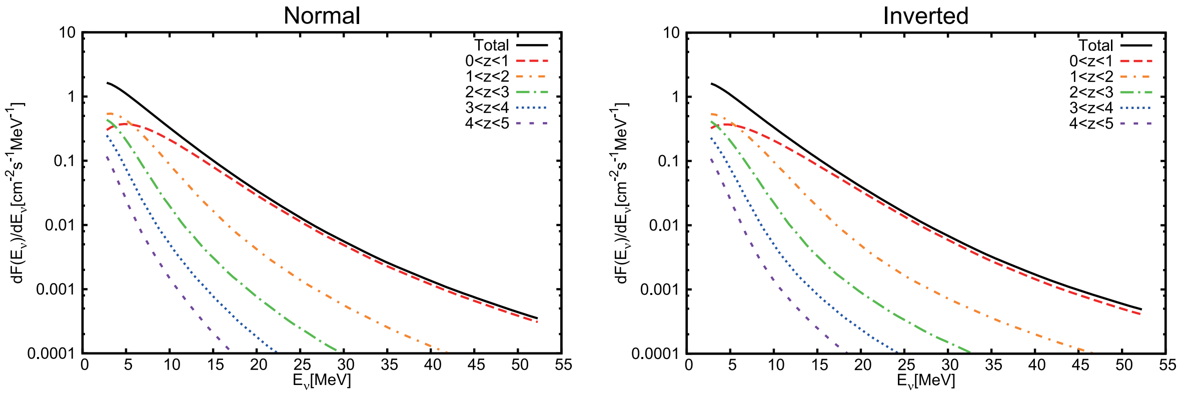

contributions from $0 < z < 1$, $1 < z < 2$, $2 < z < 3$, $3 < z < 4$, $4 < z < 5$, Nakazato *et al.*, 2015

Luminosity and spectra of SNν depend of progenitors.
Initial Mass M and metallicisty Z affect density profiles of pre-collapse cores.

$$\Rightarrow \frac{dN_\nu(E'_\nu, M, Z)}{dE'_\nu}$$

+ oscillation ($\phi^{obs}_{\bar{\nu}_e}(E) = \bar{P}\phi^{SN}_{\bar{\nu}_e}(E) + (1-\bar{P})\phi^{SN}_{\nu_x}(E)$), $\bar{P}$=0.68(NH) or 0(IH)

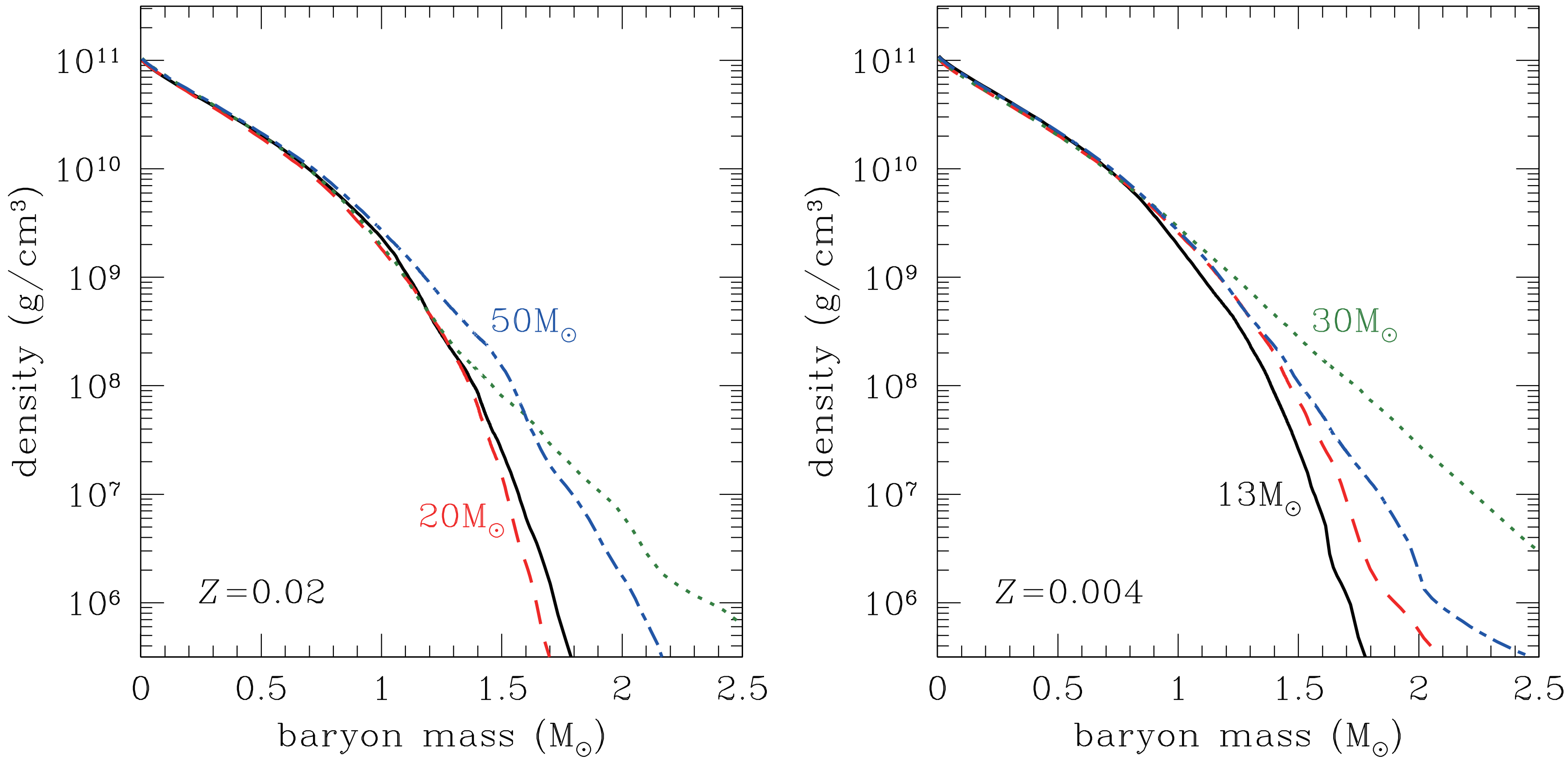

Figure 4. Density profiles at times with the central density of 10^{11} g cm^{-3} for progenitor models with metallicity $Z = 0.02$ (left panel) and 0.004 (right panel). In both panels, solid, dashed, dotted, and dot-dashed lines correspond to the models with initial mass $M_{\rm init} = 13\ M_\odot$, $20\ M_\odot$, $30\ M_\odot$, and $50\ M_\odot$, respectively.
(A color version of this figure is available in the online journal.)

Density profiles of progenitors with various M, Z : Nakazato *et al.*, 2013

Supernova rate and Cosmic Chemical Evoluton

Our model:

$$\frac{d^2 R_{\rm CC}(z,M,Z)}{dMdZ}dZdM = R_{\rm CC}(z)\psi_{\rm ZF}(z,Z)dZ\psi_{\rm IMF}(M)dM$$

Supernova (Core-Collpase) Rate

$$R_{\rm CC}(z) = \dot{\rho}_*(z) \times \frac{\int_{M_{\rm min}}^{M_{\rm max}} \psi_{\rm IMF}(M)\ {\rm d}M}{\int_{0.1M_\odot}^{100M_\odot} M\psi_{\rm IMF}(M)\ {\rm d}M}\ [{\rm yr}^{-1}\,{\rm Mpc}^{-3}]$$

Initial Mass Function(IMF): $\psi_{\rm IMF}(M) \propto M^{-2.35}$ (Salpeter type)

Star formation rate with initial mass of $M \sim M + dM$ $[{\rm yr}^{-1}] \propto \psi_{\rm IMF}(M)dM$

Cosmic Star Formation Rate Density(CSFRD): $\dot{\rho}_*(z)$ $[M_\odot\,{\rm yr}^{-1}\,{\rm Mpc}^{-3}]$

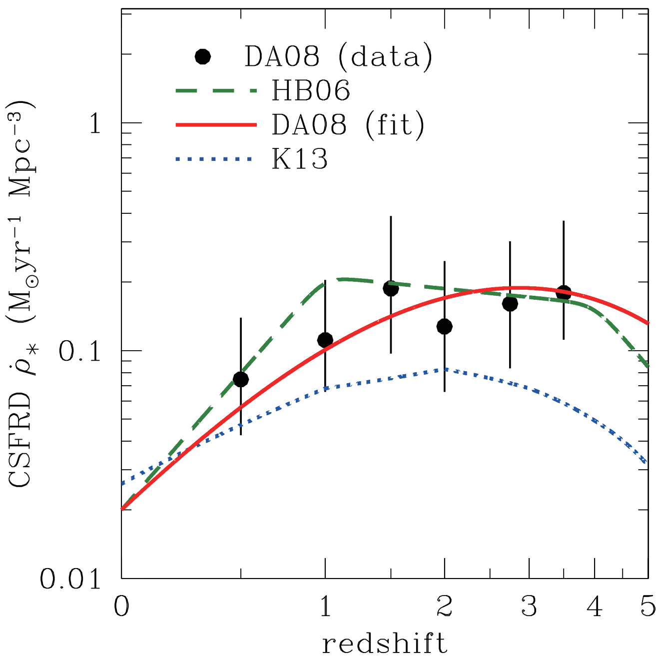

Several models of CSFRD as a function of redshift. Dashed, solid and dotted lines correspond to the models in Hopkins & Beacom'06, DA08 and Kobayashi *et al.*'13, respectively.

Evolution of Metallicity Distribution: $\psi_{\rm ZF}(z, Z)$

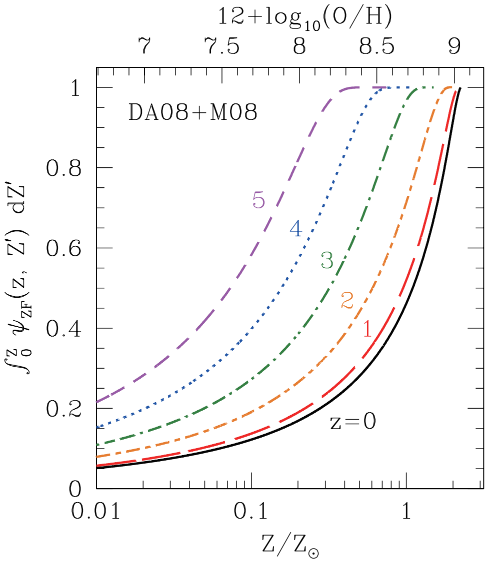

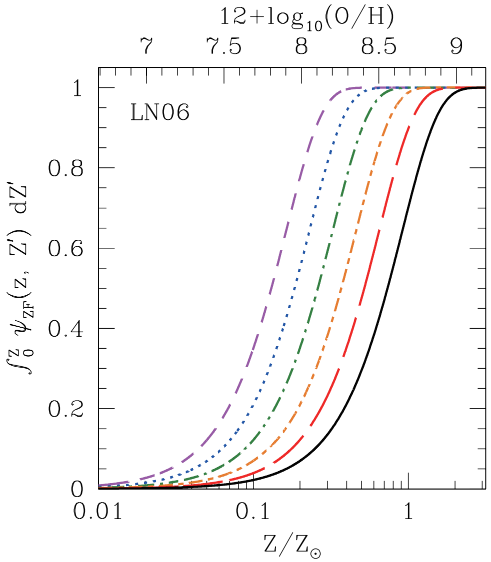

Normalized cumulative metallicity distribution function, which represents the fraction of progenitors with metallicity less than Z, for the models in DA08+Maiolino'08 (*left*) and Langer & Norman'06 (*right*). The lines correspond, from bottom to top, to redshifts of $z = 0$, 1, 2, 3, 4 and 5.

Nakazato et al.(2013) より

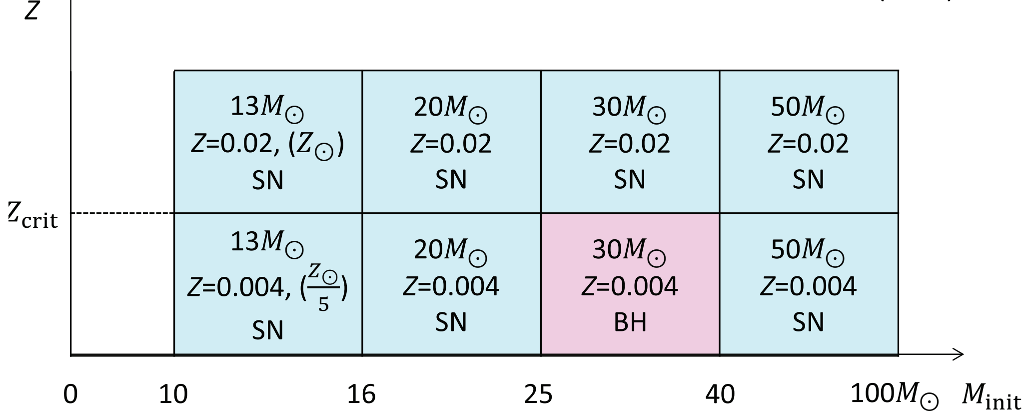

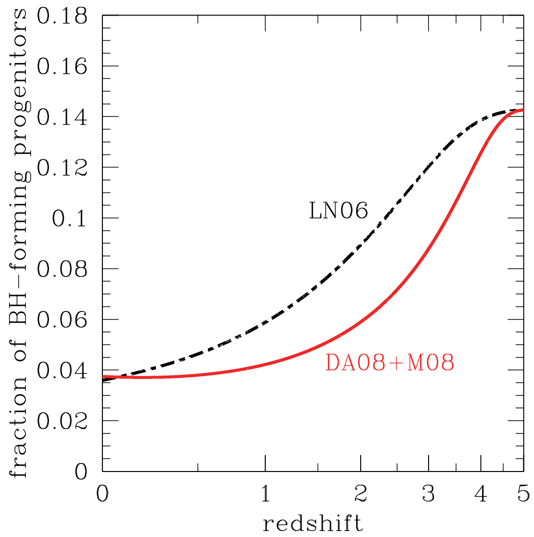

Fraction of black-hole-forming progenitors as a function of redshift. Dot-dashed and solid lines correspond to the models with the metallicity evolution of LN06 and DA08+M08, respectively. $Z_{\rm crit} \equiv \sqrt{Z_\odot \cdot 0.2 Z_\odot}$

Dependence on various models

Shock revial time: convection or SASI?

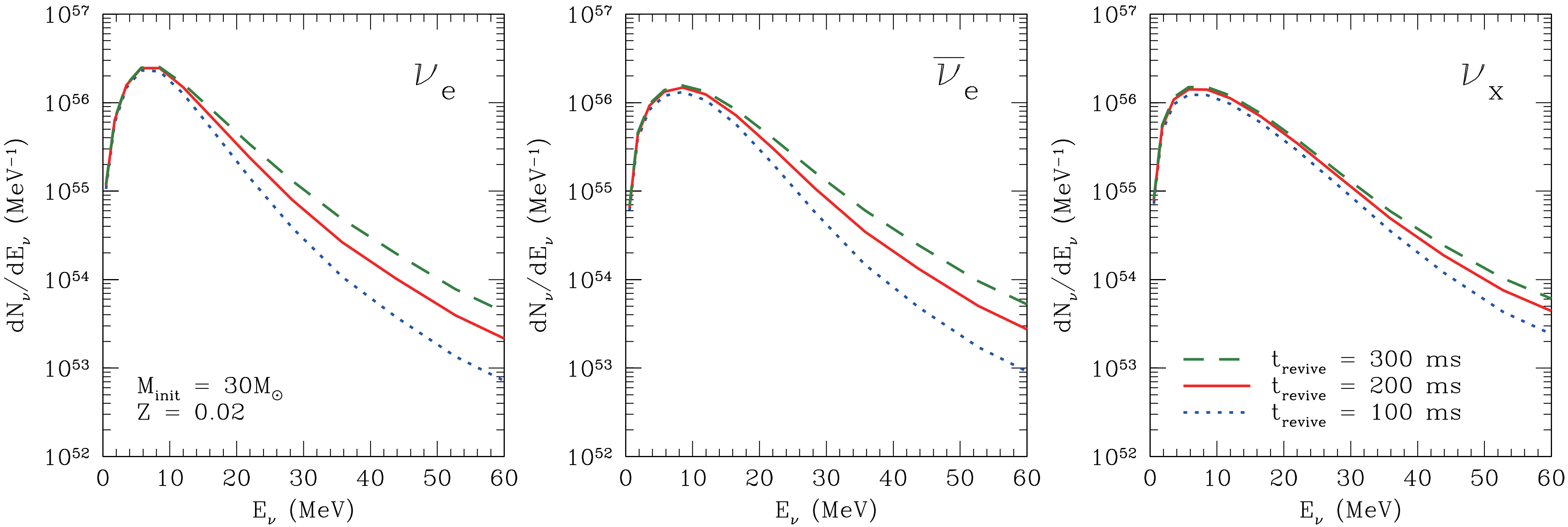

Neutrino number spectra of supernova with $30M_\odot$, $Z = 0.02$ and shock revival times of $t_{\rm revive} =$ 100 ms (dotted), 200 ms (solid) and 300 ms (dashed). The left, central and right panels correspond to ν_e, $\bar{\nu}_e$ and ν_x $(= \nu_\mu = \bar{\nu}_\mu = \nu_\tau = \bar{\nu}_\tau)$, respectively.

For models in which the shock wave revive later, the accretion phase lasts longer and therefore relatively high energy neutrinos related to the mass accretion are increased.

Shock revial time

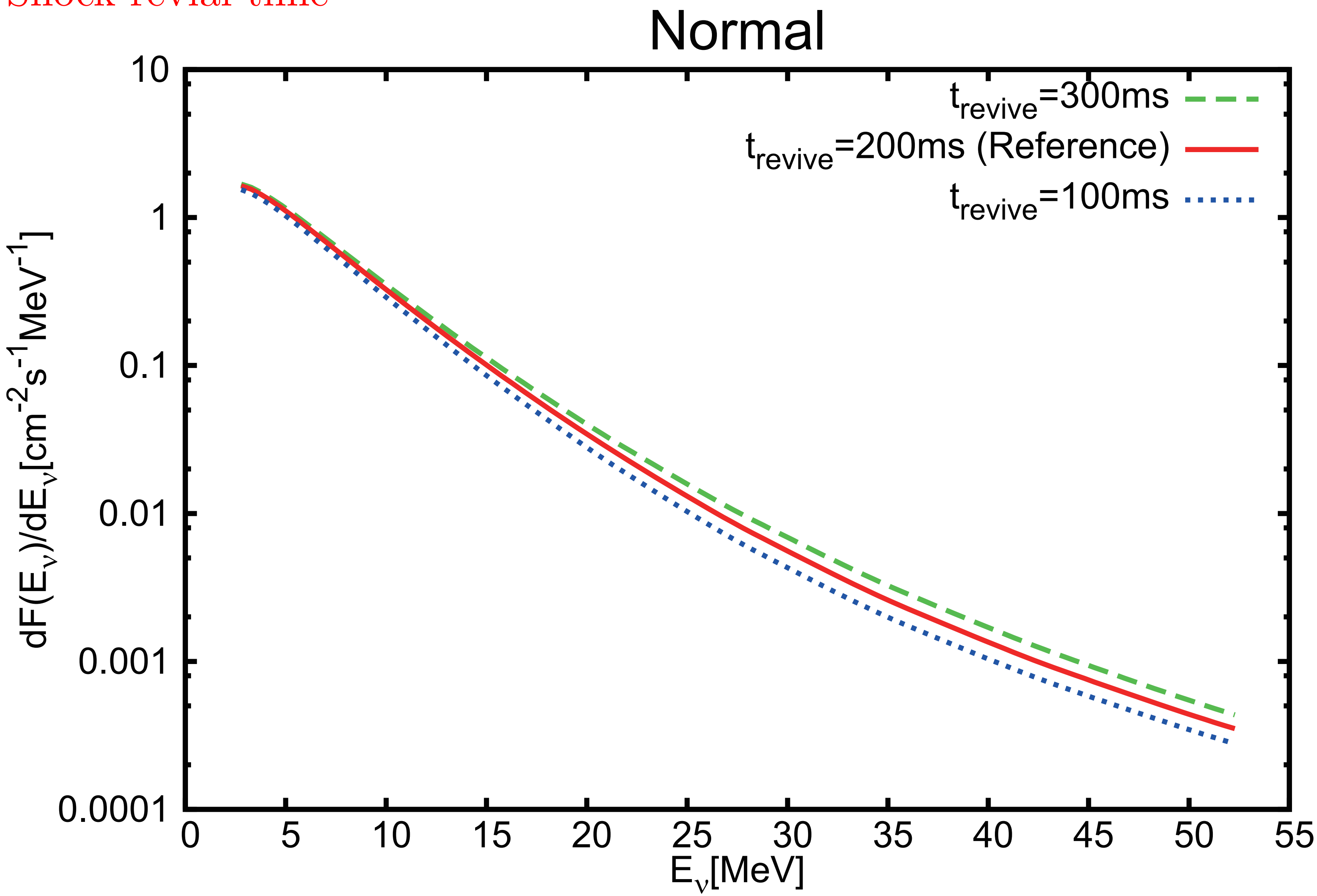

In the case of normal hierarchy (large survival probability of $\bar{\nu}_e(\bar{P} \sim 0.68)$), dependence on the shock revival time is prominent.

Neutrinos from BH forming case depend on EOS

TABLE 1
NUMERICAL RESULTS FOR BLACK HOLE FORMATION OF PROGENITOR WITH $(M, Z) = (30M_\odot, 0.004)$.

EOS	t_{BH} (ms)	$\langle E_{\nu_e} \rangle$ (MeV)	$\langle E_{\bar{\nu}_e} \rangle$ (MeV)	$\langle E_{\nu_x} \rangle$ (MeV)	$E_{\nu_e,\mathrm{tot}}$ (10^{52} erg)	$E_{\bar{\nu}_e,\mathrm{tot}}$ (10^{52} erg)	$E_{\nu_x,\mathrm{tot}}$ (10^{52} erg)	$E_{\nu_{\mathrm{all}},\mathrm{tot}}$ (10^{53} erg)
Shen	842	17.5	21.7	23.4	9.49	8.10	4.00	3.36
LS(220 MeV)	342	12.5	16.4	22.3	4.03	2.87	2.11	1.53

NOTE. — t_{BH} is the time to black hole formation measured from the core bounce. The mean energy of the emitted ν_i until black hole formation is denoted as $\langle E_{\nu_i} \rangle \equiv E_{\nu_i,\mathrm{tot}}/N_{\nu_i,\mathrm{tot}}$, where $E_{\nu_i,\mathrm{tot}}$ and $N_{\nu_i,\mathrm{tot}}$ are the total energy and number of neutrinos, respectively. ν_x stands for μ- and τ-neutrinos and their anti-particles: $E_{\nu_x} = E_{\nu_\mu} = E_{\bar{\nu}_\mu} = E_{\nu_\tau} = E_{\bar{\nu}_\tau}$. $E_{\nu_{\mathrm{all}},\mathrm{tot}}$ is the total neutrino energy summed over all species.

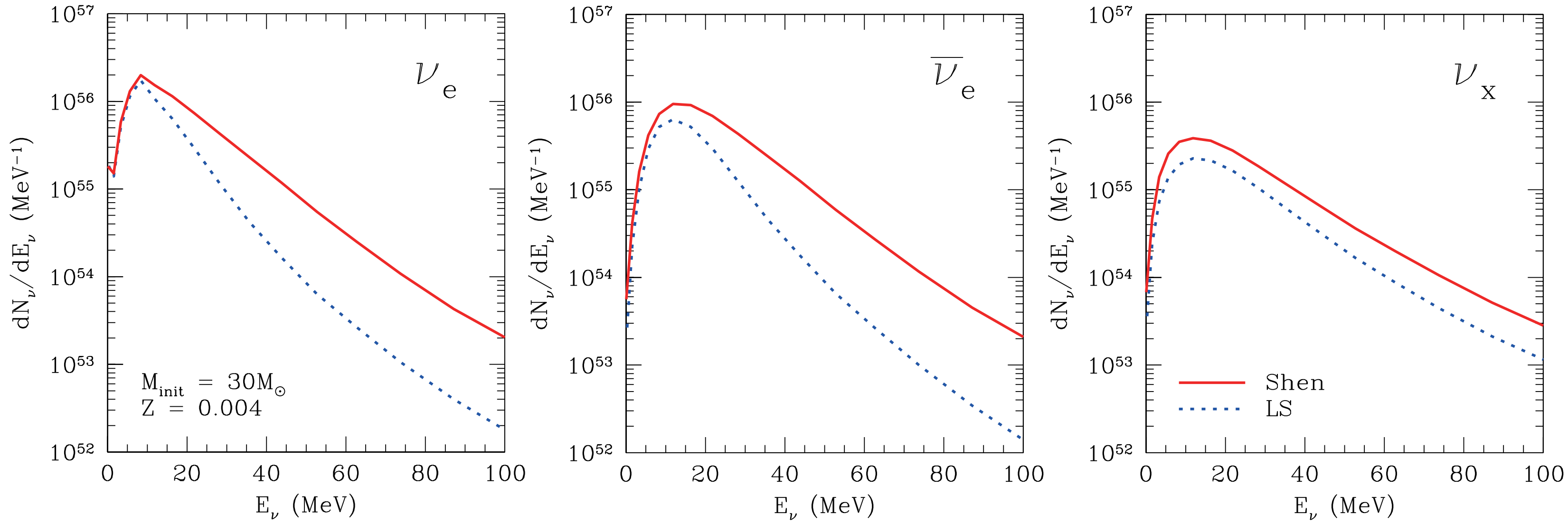

Neutrino number spectra for black hole formation with $30M_\odot$, $Z = 0.004$ and Shen EOS (solid) and LS EOS (dotted). The left, central and right panels correspond to ν_e, $\bar{\nu}_e$ and ν_x $(= \nu_\mu = \bar{\nu}_\mu = \nu_\tau = \bar{\nu}_\tau)$, respectively.

Softer EOS has smaller maximum of NS and leads to earlier BH formation. $\Rightarrow$ Shorter accretion phase, less neutrino emission

Neutrinos from BH forming case depend on EOS

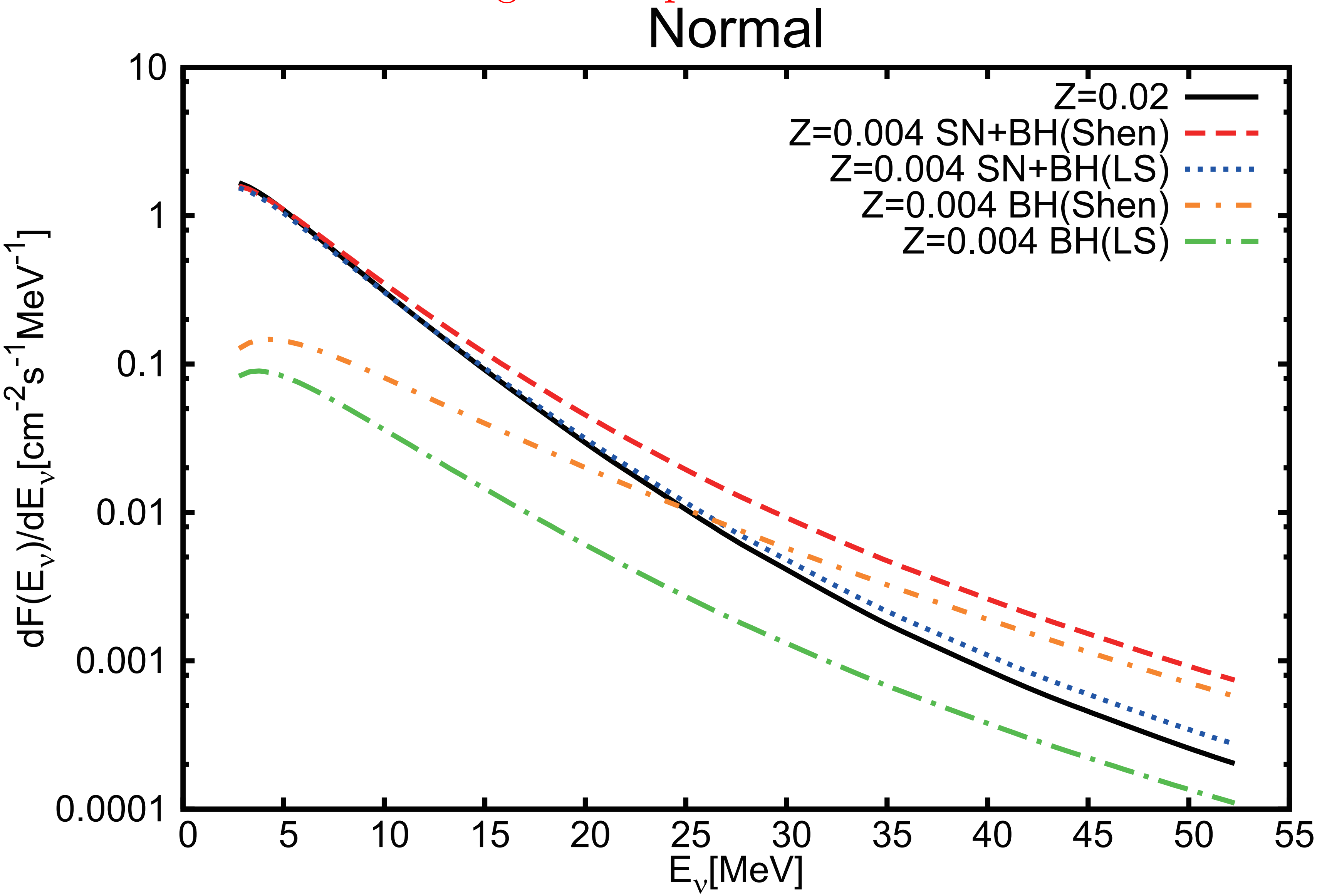

Comparison of virtual models without metallicity evolution

BH formation events contribute to high energy part of SRN.

But soft EOS resulting in too early BH formation is not the case.

Metallicity evolution : fraction of BH forming case

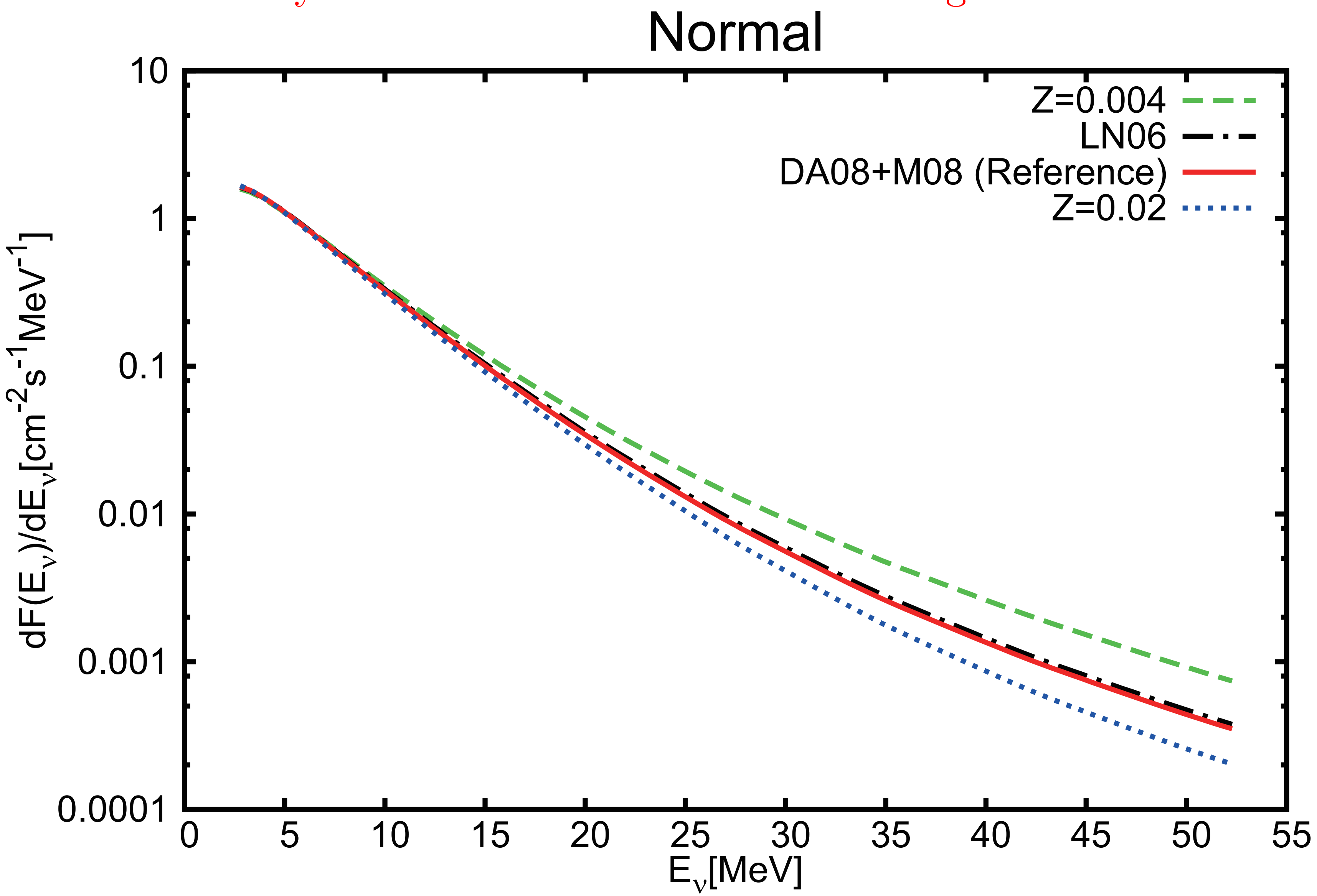

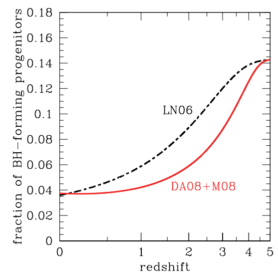

BH forming events contribute to high energy $\bar{\nu}_{\rm e}$. In the case of normal hierarchy (large survival probability of $\bar{\nu}_{\rm e}(\bar{P} \sim 0.68)$), contribution of BH formin case is prominent.

Difference between metallicity evolution models (DA08+M08 and LN06) is small.

Evolution of Cosmic Star Formation Rate Density

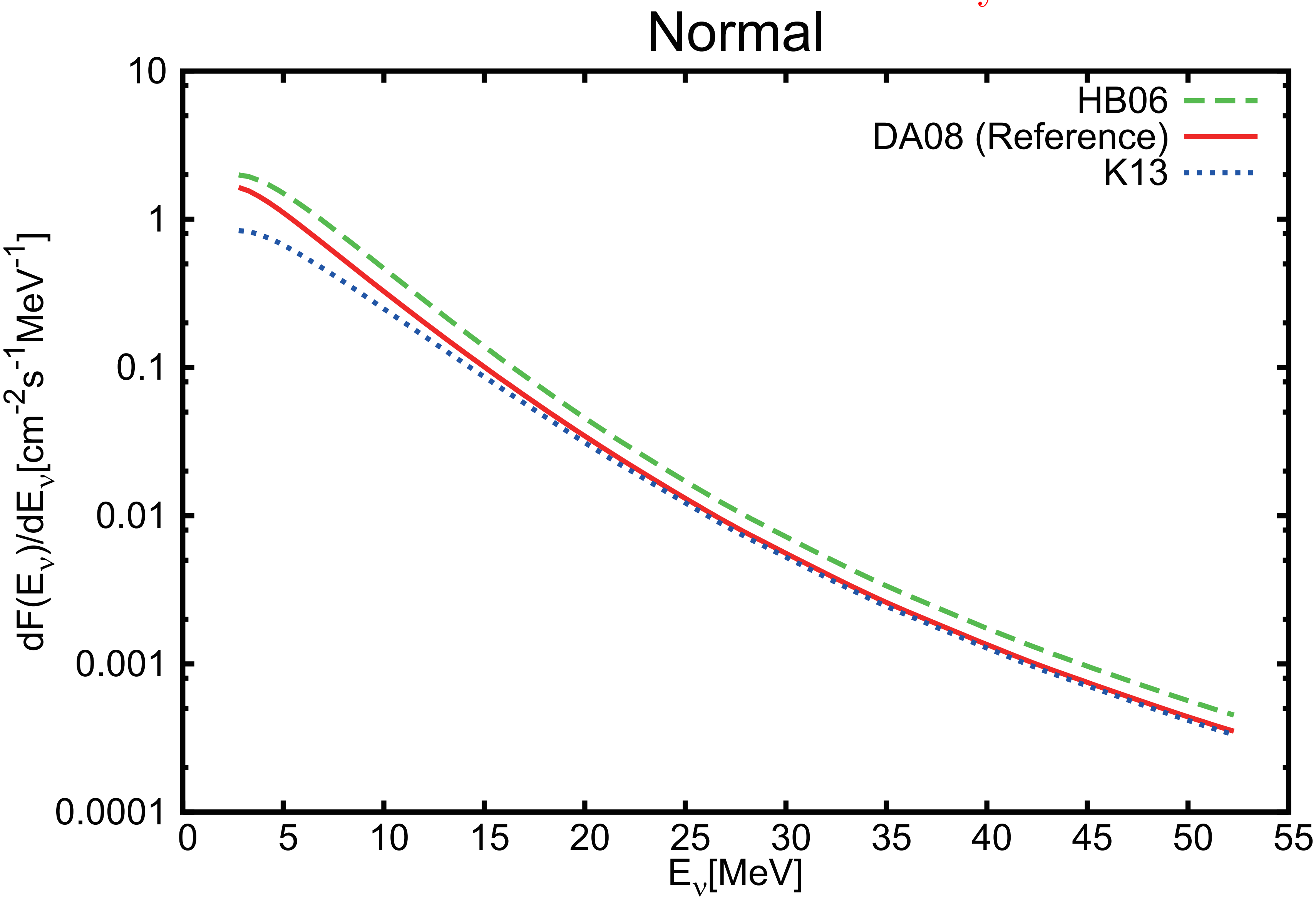

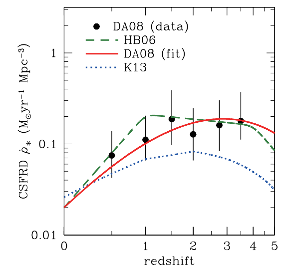

Differences among CSFRD become large at $z > 0.5$. $\Rightarrow$ influences on low energy part of SRN

Summary of model dependences

- Reference model
- lower limit model
- upper limit model

TABLE 3
SRN EVENT RATES IN VARIOUS RANGES OF POSITRON ENERGY IN SUPER-KAMIOKANDE OVER 1 YEAR (I.E., PER 22.5 KTON YEAR) FOR MODELS WITH METALLICITY EVOLUTION OF DA08+M08.

			Normal mass hierarchy			Inverted mass hierarchy			
CSFRD	t_{revive}	EOS for BH	18-26	10-18	10-26 MeV	18-26	10-18	10-26 MeV	Figure 12
HB06	100 ms	Shen	0.286	0.704	0.990	0.375	0.832	1.207	
		LS	0.227	0.635	0.863	0.351	0.806	1.156	
	200 ms	Shen	0.361	0.833	1.193	0.429	0.920	1.349	
		LS	0.302	0.764	1.066	0.404	0.893	1.297	
	300 ms	Shen	0.432	0.938	1.370	0.463	0.967	1.431	Maximum
		LS	0.374	0.869	1.242	0.439	0.941	1.379	
DA08	100 ms	Shen	0.219	0.515	0.734	0.286	0.598	0.885	
		LS	0.178	0.464	0.642	0.269	0.578	0.847	
	200 ms	Shen	0.274	0.604	0.879	0.326	0.660	0.986	Reference
		LS	0.233	0.554	0.787	0.308	0.640	0.948	
	300 ms	Shen	0.326	0.677	1.003	0.350	0.694	1.044	
		LS	0.285	0.627	0.911	0.333	0.674	1.007	
K13	100 ms	Shen	0.203	0.443	0.645	0.264	0.505	0.769	
		LS	0.171	0.410	0.581	0.252	0.492	0.744	Minimum
	200 ms	Shen	0.252	0.514	0.767	0.298	0.554	0.853	
		LS	0.221	0.482	0.703	0.286	0.542	0.827	
	300 ms	Shen	0.298	0.570	0.868	0.319	0.580	0.899	
		LS	0.266	0.537	0.804	0.306	0.568	0.874	

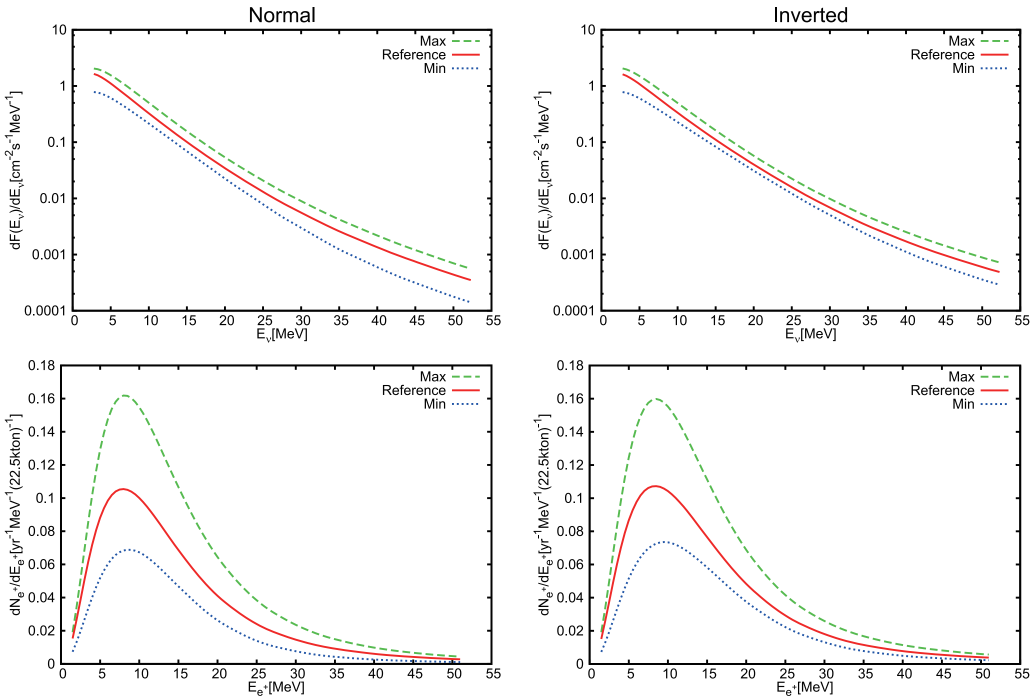

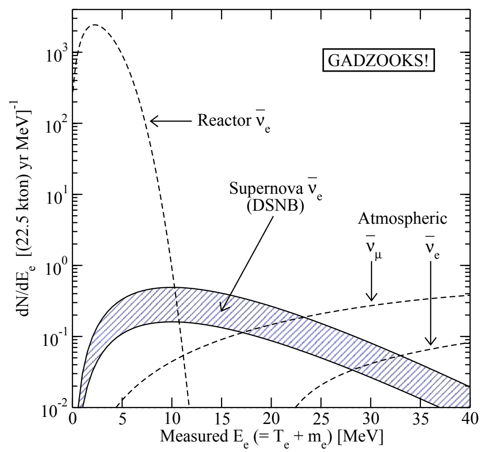

Figure 2. The expected coincident signals in Super–K with 100 tons of $GdCl_3$. Detector energy resolution is properly taken into account. The upper supernova curve is the current SK relic limit, while the lower curve is the theoretical lower bound.

Nakazato *et al.*, 2015.

Vagins, NPB PS 143(2005) 456, Fig.2

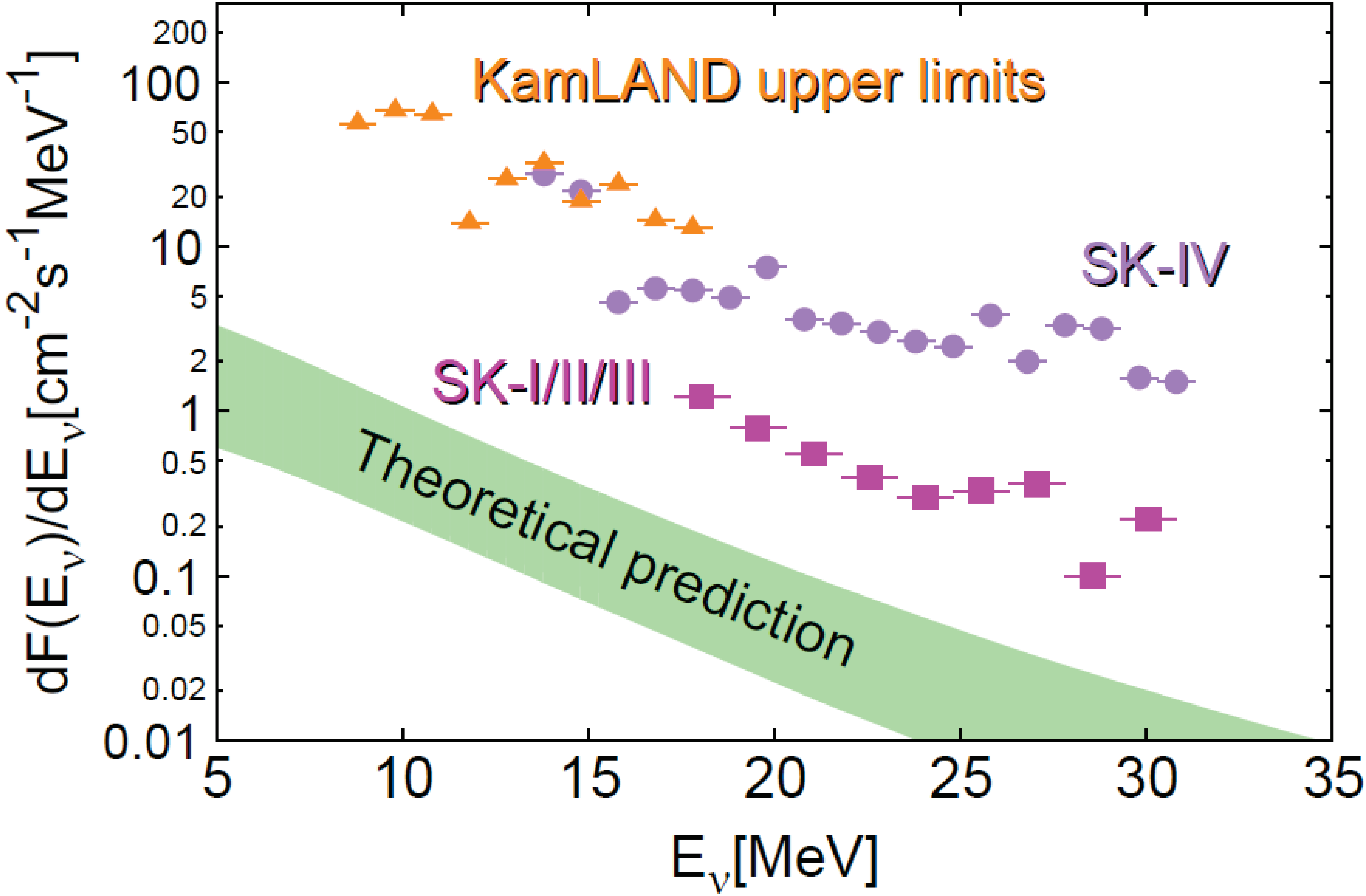

http://asphwww.ph.noda.tus.ac.jp/srn/

Togashi EOS based on the realistic nuclear force model

- EOS for uniform phase $\Leftarrow$ variational many body theory with the AV18 two-nucleon potential and UIX three-nucleon potential
- EOS for non-uniform phase $\Leftarrow$ Thomas-Fermi (TF) approximation: minimization of free energy of Wigner-Seitz cells (following Shen EOS) assuming a single representative nucleus
  $\Leftrightarrow$ Furusawa's EOS with nuclear emsemble (Liquid drop model + Nuclear Statistical Equilibrium) (Furusawa *et al.* 2017)

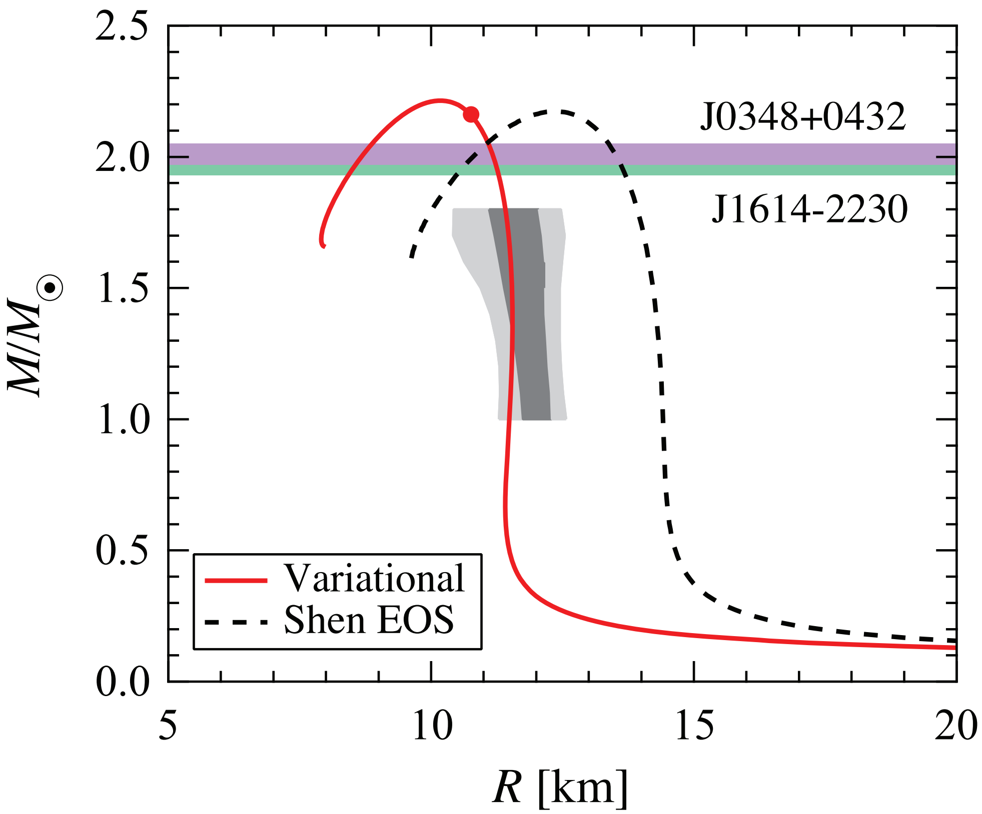

EOS	Togashi	Shen	LS220
K[MeV]	245	281	220
$E_{\rm sym}$[MeV]	30.0	36.9	28.6
L[MeV]	30	111	73.8
n_0[fm^{-3}]	0.16	0.145	0.155
E_0[MeV]	16.1	16.3	16.0
$M_{\rm NSmax}[M_\odot]$	2.21	2.23	2.06

Togashi *et al.*, Nucl. Phys. A961 (2017) 78

Consistent with GW data of the binary NS merger (GW170817)

Togashi EOS: softer than Shen EOS and smaller symmetry energy

EOS dependence of PNS cooling

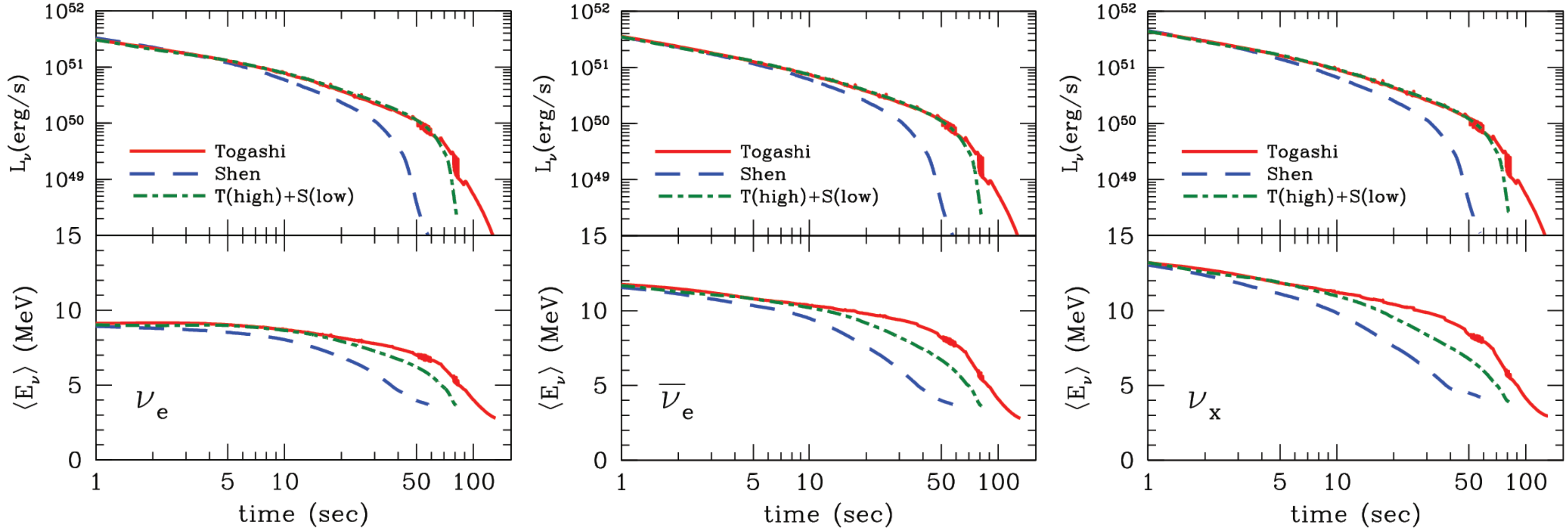

FIG. 1. Luminosities (upper plots) and mean energies (lower plots) of the emitted neutrinos as a function of time after the bounce. The panels correspond, from left to right, to ν_e, $\bar{\nu}_e$, and ν_x ($=\nu_\mu$, ν_τ, $\bar{\nu}_\mu$, $\bar{\nu}_\tau$). Solid, dashed, and dot-dashed lines are for the Togashi EOS, Shen EOS, and T+S EOS, respectively.

time scale of neutrino emission and total energy emitted by neutrinos: Togashi EOS $\sim$ T+S $>$ Shen $\Leftarrow$ Togashi EOS is softer and has a more compact PNS (Togashi EOS: R(50s)=11.8 km, $\rho_{\mathrm{B}c} = 7.73 \times 10^{14}$ g cm^{-3}, Shen EOS: R =14.1 km, $\rho_{\mathrm{B}c} = 4.87 \times 10^{14}$ g cm^{-3}).
While Togashi EOS and T+S EOS (interpolation between Togashi EOS for high density and Shen EOS for low density) are similar as for softness, neutrino mean energies at $t > 20$ s are higher for Togashi EOS than T+S EOS.
$\Leftarrow$ Crust composition

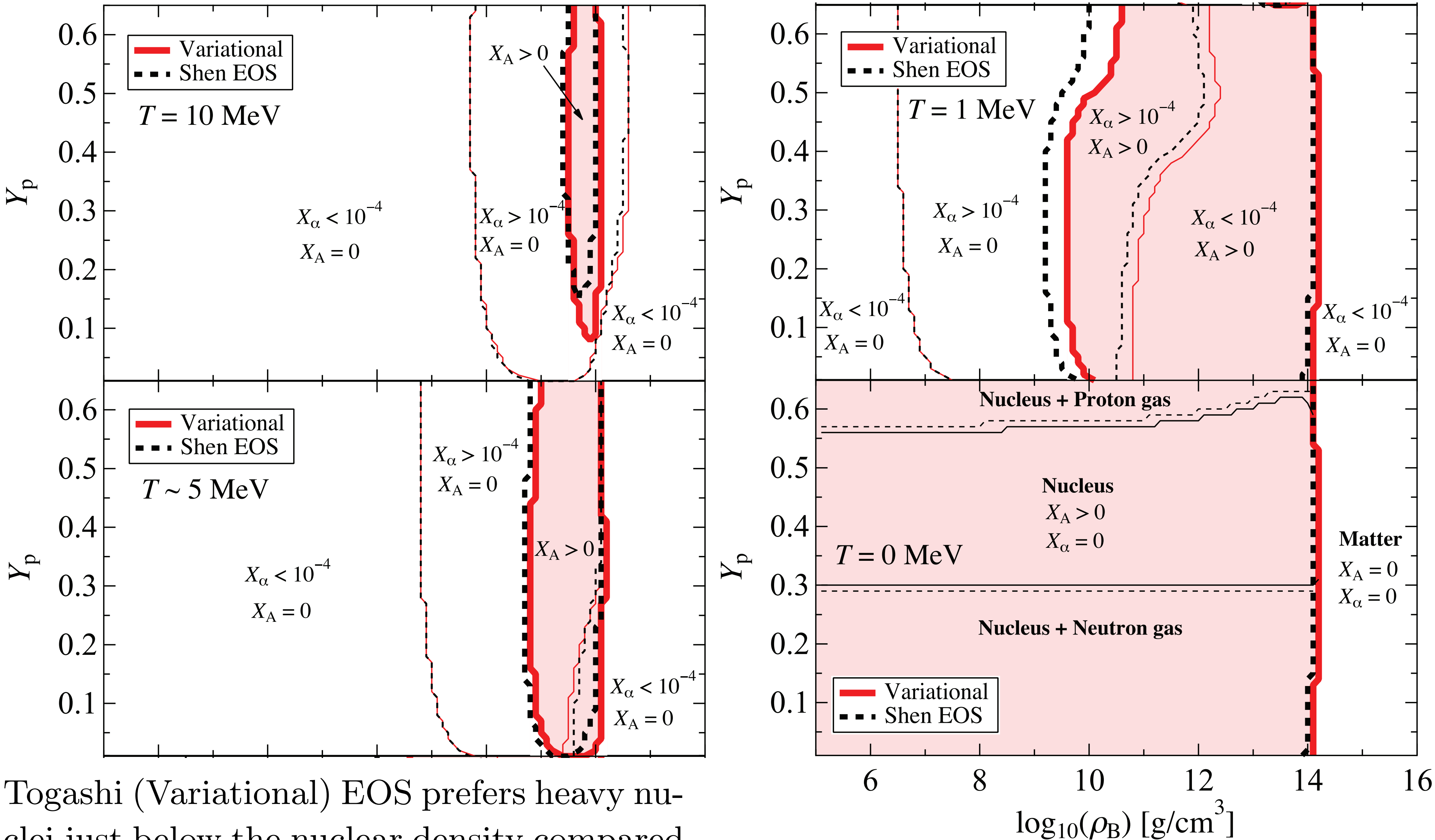

Togashi (Variational) EOS prefers heavy nuclei just below the nuclear density compared with Shen EOS.

The density derivative coefficient of the symmetry energy L: Togashi EOS ($L = 35$ MeV) $<$ Shen EOS ($L = 111$ MeV) $\Rightarrow$ Symmetry energy at subnuclear densities and proton (electron) fraction: Togashi $>$ Shen

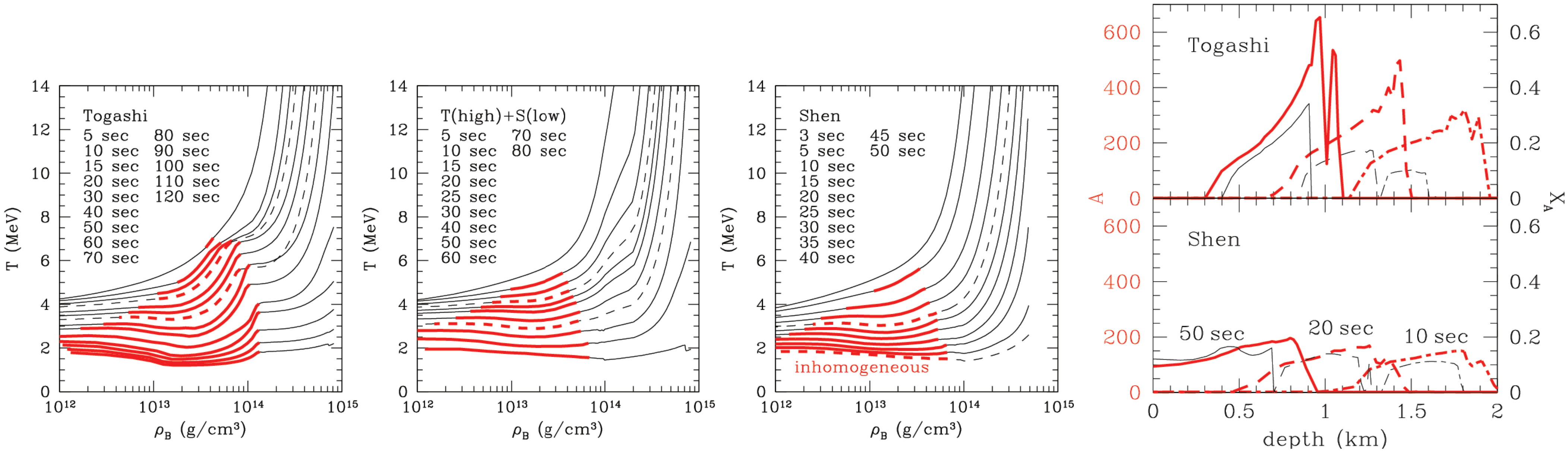

Main opacity source : coherent scattering off heavy nuclei:

$\sigma \propto A^2$, $n_A \propto \rho_{\rm B} X_{\rm A}/A$, mean free path $\lambda \propto 1/(\rho_{\rm B} X_{\rm A} A)$: $\lambda(\mathrm{Togashi}) < \lambda(\mathrm{T+S})$

For the Togashi EOS, neutrinos efficiently interact with the matter and keep the matter hot near the PNS surface. Reflecting the temperature there, the neutrino mean energy remains higher for the case with the Togashi EOS.

Summary

- We provide numerical data of the time evolution of emitted neutrino spectra obtained by our 1D models of supernova explosion and of the formation of a black hole.
  Neutrinos from failed supernovae are good probe to high density matter
- Estimation of Supernova Relic Neutrino (SRN) spectra with uncertainties on metallicity evolution, cosmic star formation rate density (CSFRD), shock revival timescale, equation of state (EOS) for high density matter
- Shock revival timescale and EOS affect the high energy part of SRN ($\bar{\nu}_{\mathrm{e}}$) (Especially for the case of normal hierachy)
- CSFRD affects the low energy part of SRN ($\bar{\nu}_{\mathrm{e}}$)
- SK with Gd might observe 4 - 9 SRN events(10-18MeV)/10years
- Togashi EOS based on realistic nuclear force potential is ready for supernova simulations.
- The neutrino luminosity and mean energy are higher and the cooling time scale is longer for the softer EOS. Meanwhile, the neutrino mean energy and the cooling time scale are also affected by the low-density EOS because of the difference in the population of heavy nuclei. Heavy nuclei have a large scattering cross section with neutrinos owing to the coherent effects and act as thermal insulation near the surface of a PNS. The neutrino mean energy is higher and the cooling time scale is longer for an EOS with a large symmetry energy at low densities, namely a small density derivative coefficient of the symmetry energy, L.